Charles University

Faculty of Science

Department of physical geography and geoecology

Variabilita množství stabilních izotopů vody ve sněhu

Water stable isotopes variability in snowpack

Bachelor’s thesis

Jan Kopečný

Supervisor of the thesis: doc. RNDr. Michal Jeníček, Ph.D.

Praha 2024

Objectives of the bachelor's thesis

The topic of the thesis:

Water stable isotopes variability in snowpack

Objectives of the work:

1.) Assessment of the current state of research on the role of the physical properties of snow in snowmelt runoff, its progression, and extremity during various types of melting events.
2.) Analysis of the temporal and spatial variability of snow properties in a selected mountainous locality using measurements of physical characteristics and the concentration of stable water isotopes in individual snow layers.

Methods, Area of Interest, Data Sources

The first part of the work will focus on a literature review and assessment of the current state of research on the role of the physical properties of snow in snowmelt runoff, its progression, and extremity during various types of melting events, including an evaluation of past and future changes in these events due to changes in vegetation and climate.

The analytical part of the work will evaluate the temporal variability of the physical properties of snow in different horizons within a selected locality using snow profile analysis on open areas and vegetation. Regular measurements (approximately every 3 weeks) of physical characteristics of individual snow layers (such as height, density, temperature, snow hardness, etc.) are anticipated, along with the collection of snow samples from various horizons for subsequent analysis of 2H and 18O isotope content. Beyond these analyses, there is also the potential to relate the isotopic properties of the snow to those of meltwater, which will be collected using a snow lysimeter.

Date of Assignment: 5.12.2023

Name of the student: Jan Kopečný

Student's Signature: .....Jan Kopečný .....

Supervisor's Name: doc. RNDr. Michal Jeníček, Ph.D.

Supervisor's Signature: **.....**

Declaration

I declare that I have independently worked on this bachelor's thesis and that I have properly cited all the sources used. I agree to the loan of this thesis for study purposes and consent to its proper inclusion in the library's collection.

Prague, July 31, 2024 ……..…….....

Jan Kopečný

Poděkování:

Tímto bych rád poděkoval Michalu Jeníčkovi za mnoho cenných rad
a velké množství času stráveného při vedení této práce. Dále bych rád poděkoval Dominiku Míkovi a Lukáši Vlčkovi za pomoc během sběru dat v terénu a pomoc s laboratorním zpracováním dat a interpretaci výsledků.

Abstract:

Stable water isotopes are used as a natural tracer for hydrograph separation, allowing for distinction between various water sources. Snow isotopic composition can be influenced by a number of meteorological, hydrological, and physical processes. A better understanding of how snow water isotopes change during the snowmelt process can improve hydrograph separation methods and provide insight into the processes that influence snowmelt and the resulting runoff. During the winter season of 2024, four snow pits were conducted at the Ptačí brook in the Šumava Mountains. The physical properties of the snow, such as snow water equivalent, hardness, grain type and temperature, were measured at approximately 3-week intervals. In addition, samples of stable water isotopes in the snow, specifically $^{18}O/^{16}O$ and $^{2}H/^{1}H$, were taken from identified stratigraphic layers. It was found that the snow depth in the open plot was, on average, 54% higher than in the forest plot, and the snow water equivalent was, on average, 36% higher in the open plot than in the forest plot. The open plot snowpack showed greater physical and isotopic stratigraphic heterogeneity as well as increased depletion in heavy isotopes, in comparison to the forest snowpack. The isotopic samples from the open site snowpack varied between δ^{18} O = -20.37‰; $\delta^{2}H$ = 154.28‰ and $\delta^{18}O$ = -9.79‰; $\delta^{2}H$ = -70.09‰, while the forest samples varied between $\delta^{18}O$ = -14.67‰; $\delta^{2}H$ = -110.86‰ and $\delta^{18}O$ = -9.24‰; $\delta^{2}H$ = -65.33‰. The stratigraphy of the open site snowpack remained relatively stable even after the occurrence of rain-on-snow events. Furthermore, the melting of layers was observed to occur without isotopically affecting adjacent layers below, indicating the occurrence of lateral flow patterns.

Key words: snow water isotopes, snow water equivalent, snow profile, physical properties of snow

Abstrakt:

Stabilní izotopy jsou používány jako přírodní stopovače umožňující separaci hydrogramu. Protože izotopové složení sněhu může být ovlivněno různými meteorologickými, hydrologickými a fyzikálními procesy, podrobnější porozumění tomu, jak se vyvíjí poměr stabilních izotopů ve sněhové pokrývce během tání, by mohlo pomoci lépe odlišit jednotlivé složky odtoku, ale také porozumět procesům, které sněhový odtok ovlivňují. Během zimní sezóny 2024 byly v povodí Ptačího potoka na Šumavě provedeny čtyři měření po přibližně třech týdnech. Ve sněhových profilech bylo změřeno SWE, tvrdost sněhu, typ sněhu a teplota sněhu. Dále byly z každé identifikované vrstvy odebírány vzorky stabilních izotopů ($^{18}O/^{16}O$ a $^{2}H/^{1}H$). Výška sněhu na otevřené ploše byla v průměru o 54 % vyšší než v lese a vodní hodnota sněhu na otevřené ploše dosahovala v průměru o 36 % vyšších hodnot než v lese. Sníh na otevřené ploše vykazoval oproti lesní pokrývce vyšší fyzikální i izotopovou heterogenitu. Ve srovnání se sněhem v lese byla sněhová pokrývka na otevřené ploše také více ochuzena o těžké izotopy. Na otevřené ploše se poměr izotopů pohyboval mezi: $\delta^{18}O$ = -20,37‰; $\delta^{2}H$ = -154,28‰ a $\delta^{18}O$ = -9,79‰; $\delta^{2}H$ = -70,09‰, zatímco v lese byly hodnoty následující: $\delta^{18}O$ = -14,67‰; $\delta^{2}H$ = -110,86‰ a $\delta^{18}O$ = -9,24‰; $\delta^{2}H$ = -65,33‰. Izotopové složení sněhu na otevřené ploše bylo v průběhu měření relativně stabilní i přes zaznamenané dešťové události ROS. Tání vrchních vrstev sněhu poté často neovlivnilo izotopové složení spodních vrstev. To naznačuje odtok ze sněhové pokrývky pomocí preferenčních odtokových cest zvaných lateral flow.

Klíčová slova: stabilní izotopy sněhu, vodní hodnota sněhu, sněhový profil, deuterium, ^{18}O

Contents

1 Introduction

Snow is intrinsic to many aspects affecting life around the globe. More than 1/6 of the global human population relies on snow-covered glaciers and seasonal snow runoff as a water supply (Barnett et al., 2005). The seasonal snow that accumulates on the ground during winter acts as a temporary freshwater storage, releasing water at a later point in the season. Therefore, accumulated snow plays a significant role in ecology (Hannah et al., 2007), hydropower and agriculture (Barnett et al., 2005). However, snow processes are also associated with number of natural hazards such as floods (McCabe et al., 2007), avalanches (Baggi & Schweizer, 2009) and flush flows (Clark & Seppala, 1988). As climate change alters precipitation patterns such as accumulation amounts and snow distribution (Marty et al., 2017), rain-on-snow (ROS) events (Beniston et al., 2018) and vegetation structure (Overpeck et al., 1990; Walsh et al., 2019), runoff volumes are being simultaneously influenced (Veatch et al., 2009; Musselman et al., 2018). Thus, understanding process that drive snowpack melt and the contribution of snow to the hydrological cycle is crucial to secure benefits and minimize hazards associated with snow.

The stable isotopes of the water molecule ($\delta^{18}O$ and $\delta^{2}H$) have been commonly used as natural tracers for hydrograph separation (Klaus & McDonnell, 2013). However, the identification of snow fraction in runoff is facing challenges as snow water isotopes show great spatial (von Freyberg et al., 2020) and temporal variability (Taylor et al., 2001). Further, many physical processes have been shown to change isotopic composition of a snowpack, possibly affecting snow generated runoff. Yet few studies have focused on the temporal evolution of snowpack stable water isotopes (Evans et al., 2016). Of the few studies conducted, Juras et al. (2017) demonstrated the temporal complexity of liquid water percolation through a snowpack, resulting in different runoff volumes of different fractions of snowmelt and incoming liquid water during ROS events. Moreover, Zhou et al. (2008) described the changes caused by melt-freeze cycles, while Taylor et al. (2001) found that snow metamorphism and melt caused snowpack gradual enrichment in heavier isotopes. Evans et al. (2016) then described potential effects of snow sublimation on isotopic composition of snow and identified lateral flow mechanism of meltwater leaving the snowpack, which results in variability in snow runoff isotopic values during the winter season.

Despite these findings, there are nonetheless gaps in our scientific understanding of how snow isotopes change over time. The objective of this work is therefore to map temporal and spatial variations of snow properties and snow stable water isotopes in detail.

1.1 Objective of the research and research hypothesis

The objectives of this thesis are as follows:

1) To evaluate the current state of research on the role of the physical properties of snow in snowmelt runoff, its course, and extremity during different types of snowmelt events.

2) To analyze the temporal and spatial variability of snow properties at selected mountainous locations through the measurement of physical characteristics and the concentration of stable water isotopes in individual snow layers.

This thesis sets out the following research hypothesis:

1) The snowpack under a forest canopy has distinct physical and isotopic properties compared to the open site snowpack, with considerably lower SWE, and snow is significantly more enriched in stable water isotopes under the forest canopy.

2) Temporal isotopic evolution of the snowpack shows a gradual depletion in light water isotopes during the melting period.

1.2 Structure of the thesis

The first part of the thesis focuses on a literature review of the current state of research on the physical properties of snow related to snowmelt runoff, and its extremity during different types of snowmelt events. Additionally, past and future changes in these events due to vegetation and climate changes are discussed. The second part describes the methods and results of the research conducted in the Ptačí brook basin in the Šumava Mountains. In the final part, the results are compared with existing research.

2 Review of the role of snow in runoff generation

2.1 Physics of snow

2.1.1 Water molecule and ice crystal

The physical properties of snow and ice are largely dictated by the molecular structure of water and by the nature of the hexagonal structure of ice crystals. Water molecules are made up of by two hydrogens and a single oxygen molecule with different electronegativity between its atoms, causing the dipolarity of water molecules. Dipolar water molecules are attracted to each other by electrostatic forces known as hydrogen bonds. These bonds contribute to the unique properties of water as adhesivity and its relatively high melting and boiling point. The strength of hydrogen bounds is the strongest in ice and weakest in water vapor (DeWalle & Rango, 2008).

Water molecules have a triangular shape with an angle between H-O-H of about 104.5° for liquid water and 109° for the hexagonal ice lattice. It is the larger angle between the molecules giving the ice form of water lower density than its liquid form. The Ice density around 0°C is about 910-920 kg m^{-3} while commonly used of water density is 1000 kg/m^3, which is the density of water at 4°C (DeWalle & Rango, 2008).

2.1.2 Formation of snow crystal

Snowflakes typically have a hexagonal symmetric shape due to the molecular structure of ice Ih, which is often referred to as normal ice, occurring in nature. The process of snow particle formation starts with the freezing of a water droplet. For this process to occur super-cool water droplets and nuclei bodies of dust or other aerosols are needed. The initial crystal has a hexagonal shape and tends to grow from its edges forming the known snowflake shape (DeWalle & Rango, 2008). The shapes of crystals were first studied by Nakaya (1954) who described the shape's dependence on temperature and supersaturation in clouds (Fig.1). This diagram depicts shapes formed in a pressure of 1 013.25 hPa referred to as natural crystals.

As some nuclei bodies are better than others, ice crystals and water droplets both coexist in the cloud (Libbrecht, 2005). The saturation vapor pressure is higher over the microscopic water droplets than over the ice crystal, causing water vapor transport to the crystal and consequently crystal growth (DeWalle & Rango, 2008). Faceting will first create a simple hexagonal structure; characteristic branches are formed later as the crystal growth is limited by diffusion (Libbrecht, 2005). The morphology of the ice crystal and its microscopic shape, plays a role in the characteristics of later accumulated snow (Hu et al., 2024), where less complicated ice crystals result in a snowpack with decreased hardness. The snow morphology can influence properties of the snowpack such as porosity and liquid water content (Hu et al., 2024).

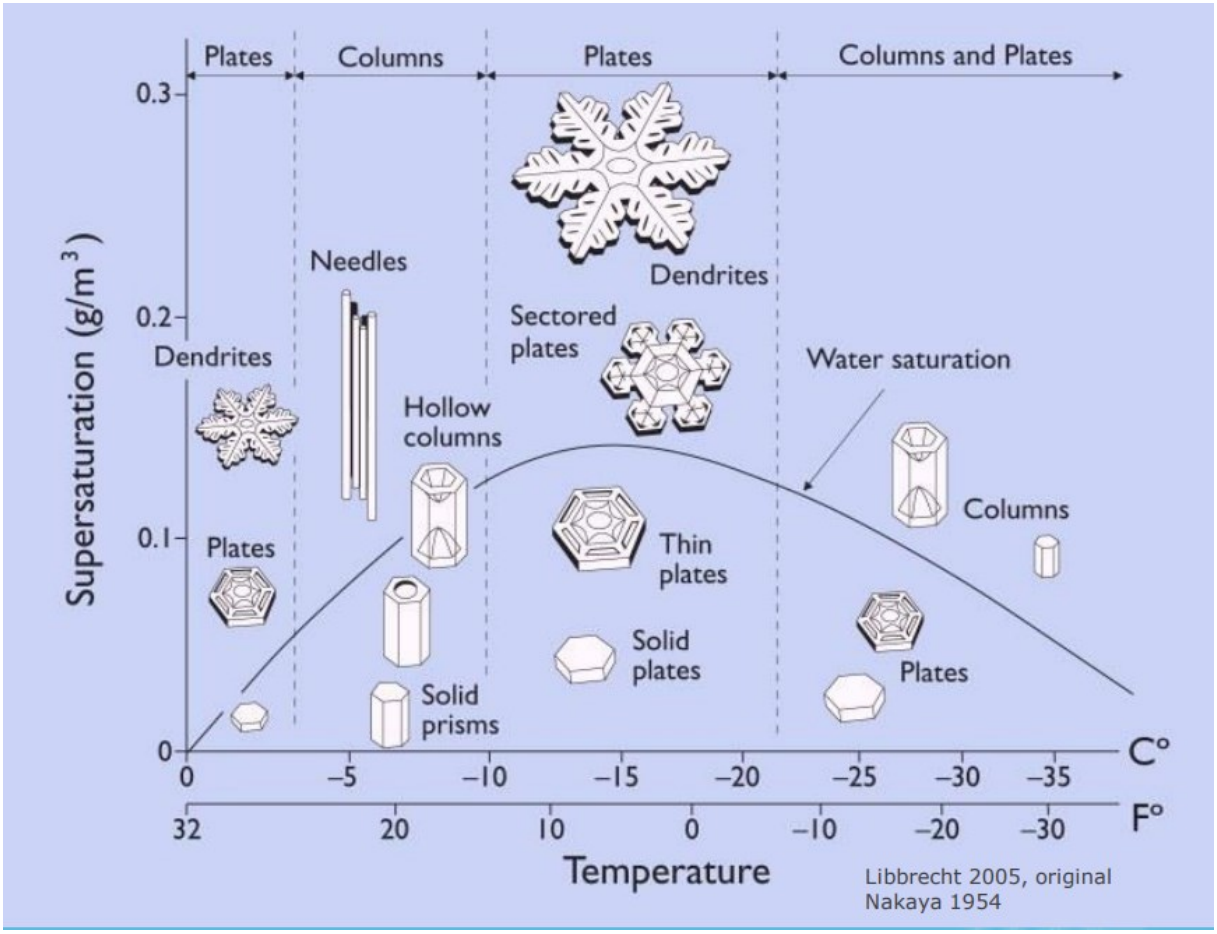

Figure 1: Snow crystal morphology diagram of crystal shape in dependence of temperature and water supersaturation. (Nakaya, 1954; Libbrecht, 2005)

2.1.3 Snow metamorphism

Seasonal snow is undergoing a continuous transformation of the size and shape of crystals (Bouvet et al., 2022) resulting in changes in temperature, density, and liquid water content of snow and other mechanical properties. These attributes determine the amount of water stored in snow or the intensity at which the snow is going to melt (Bouvet et al., 2022).

Metamorphism starts immediately after snow deposition on the ground. The first phase is the accumulation phase, where layers buried deeper in the snowpack become denser, increasing SWE (DeWalle & Rango, 2008). With increased solar radiation the snowpack's temperature then grows, eventually becoming isothermal, where the temperature over the whole snow profile is 0°C. This process is referred to as the warming phase (Seibert et al., 2015a). The last snow phase is melting. It occurs when the snow liquid water capacity of a snowpack is exceeded. At this point, any further input of energy is used for phase changes accelerating the melting process. Before melting, snow can hold a significant amount of water. Up to 10% of its SWE can be held by capillary uplift (Seibert et al., 2015a).

Throughout the snowpack's existence, snow crystals undergo changes mostly induced by pressure, humidity, and temperature changes (DeWalle & Rango, 2008). There are three main metamorphic processes within a snowpack. The first one is equi-temperature metamorphism (ETM). This type of metamorphism appears when the snowpack is in a quasi-isothermal condition and the temperature gradient over the profile is weak, causing water vapor diffusion. Water pressure is higher over convex, high-curvature surfaces but lower over concave low-curvature surfaces. This gradient causes water to sublimate over high-curvature surfaces and deposit over low-curvature surfaces, resulting in the rounded shape of crystals (Bouvet et al., 2022). The process is accompanied by the rearrangement of grains that results in a denser, stable snowpack (Seibert et al., 2015a). Snow grains formed by this type of metamorphism are internationally classified as "*rounded grains"* (RG) (Fierz et al., 2009). Commonly, ETM tends to appear in late winter and spring where air temperature and radiation increase.

Second, basic metamorphism is driven by the vertical temperature gradient commonly found in shallow snowpacks, since the isolation effect of the snow is still insignificant (DeWalle & Rango, 2008). This gradient causes higher vapor pressure in the warmer layer leading to vapor diffusion (DeWalle & Rango, 2008). Since the snowpack temperature is typically higher near the ground and lower at the surface, the vapor flux leads upwards, causing depletion of mass for crystals located deeper in the snowpack (Seibert et al., 2015a). On the other hand, vapor migrating up refreezes and creates a layer known as facet snow (Fierz et al., 2009). Facet snow is notorious for its mechanical instability making it prone to avalanche slides. Weak facet layers can be found on the bottom of the snowpack (depth hoar) as well as in the middle (facets) or on top (surface hoar) (Jamieson, 2006).

The last major metamorphic process in seasonal snowpacks is wet-snow metamorphism. Smaller grains require less heat to melt than larger grains (DeWalle & Rango, 2008). New liquid water from the smaller grains then refreeze around the large grains causing them to grow in mass (Seibert et al., 2015b). Another process is due to the pressure of an adjacent snowpack, where under higher pressure the melting point of ice grain bonds decreases, leading to melting of the bonds between ice grains. Such fusion causes mechanical instability but increases snowpack density (DeWalle & Rango, 2008). Melt-freeze processes like these are tied to the end of the snow season, occurring typically in spring or later winter, or in perennial snow cover.

2.1.4 Effects of snow metamorphism and melt on isotope composition.

Phase changes within a snowpack cause isotope transport and either depletion or enrichment of the remaining matter. In a snowpack, processes affecting isotope composition are melting and freezing of water as well as vaporization and exchange of water with soil (Carroll et al., 2022). In earlier studies, it was proposed that isotope changes due to metamorphism are tied to the very surface layers of a snowpack (Beria et al., 2018). Recent studies, however, have shown that metamorphism leads to isotope variance changes throughout the snowpack (Beria et al., 2018).

Studies done on sites in California mountains suggest that isotopic variance had decreased during the snow life cycle (Taylor et al., 2001). Fresh snow had the highest variability in isotope composition whereas late, melting snow generating runoff had the lowest variability in isotopic composition (Taylor et al., 2001). Events et al. (2016) in their study on isotope changes affected by water percolation and diffusion suggest that water pervasive flow induces a downward advection of the isotopic composition. In contrast, sublimation from the surface cause upward advection of the isotopic composition. As water percolates through the snowpack, it goes through cycles of refreezing and melting. Any refreezing that occurs then enriches the solid phase of a snowpack in heavier isotopes causing the mentioned shift of isotope layers. Processes like diffusion and dispersion lead to rather a homogenous variance of the snowpack composition (Evans et al., 2016). It is noteworthy that even though the arrangement of heavy isotope enriched and depleted layers changes in an inertial snowpack, the bulk amount of $\delta^{18}O$ or $\delta\ ^{2}H$ does not change until the liquid water or water vapor leaves the snowpack (Evans et al., 2016).

In the case of meltwater leaving, the residual snow is enriched in heavier isotopes, with a stable water isotope ratio closer to rainwater. A common observation is that the snowpack is getting enriched in heavier isotopes as the season progresses (Ala-aho et al., 2017;Taylor et al., 2001). This effect, sometimes referred to as "*melt-out-effect"* (Beria et al., 2018), is caused by the preferential melting of isotopically lighter snow, which then leaves the snowpack enriched in heavier isotopes (Taylor et al., 2001). More importantly, the "melt-out" also causes the melted water to be isotopically heavier as the season progresses. This effect was demonstrated by Ala-aho et al., (2017), where the increase of heavier isotopes from beginning to end of snowmelt was 3.5–5.6 ‰. Diurnal variations are also typical for the isotope composition as high mid-day solar radiation produces meltwater more enriched in heavier isotopes and caused by the abundance of heat, preventing refreezing of meltwater. Therefore, the depletion in heavier isotopes grows (Taylor et al., 2001). All listed variances are important for any water origin tracking as they change the "footprint" of snow in streamflow. However, the physical mechanisms behind the described effects are not fully understood (Beria et al., 2018).

2.2 Snow melt

Snow melting is a complex phenomenon affected not only by environmental features such as topography, atmospheric conditions, or vegetation but also by the physical properties of the snowpack (Hotovy & Jenicek, 2020). These properties define how snowpack reacts to excess energy inputs like radiation, turbulent heat fluxes or latent heat brought by rain events (Juras et al., 2021). Further, these physical attributes determine the intensity with which meltwater is released from the snowpack or in other words the amount of released water per unit of energy. The melt rate is then defined as the snow water equivalent (SWE) lost per unit time (usually a day) (Würzer et al., 2016). Melt rate is generally determined by the environment the physical properties of the snowpack, while the amount of released water is function of prior snow accumulation, measured as peak SWE (Hotovy & Jenicek, 2020).

Since snow melt is a crucial aspect of river regimes, understanding the effects that snow physical properties hold is essential for fields like agriculture or flood risk management (Stewart et al., 2004; Thackeray et al., 2019). In the following sections, selected aspects of physical properties of snow are discussed with review of current research and application in modeling. Next, effects induced by the environment like rain or vegetation cover are discussed.

2.2.1 Cold content

Before snowmelt can begin, a snowpack must overcome an energy deficit to release liquid water. This deficit is expressed as a cold content (C_C, [mm]) which is the total amount of liquid water that would have to refreeze in the snowpack to warm it up to 0°C throughout the vertical profile (DeWalle & Rango, 2008). Before this condition is met, any snowmelt that occurs on the surface is going to re-freeze in subsequent layers. It is therefore a key indicator of the snow melt process and more importantly its timing (Jennings et al., 2018). The relationship is described in Equation 1:

$$Cc = 1000 \frac{\rho s \cdot c \cdot d \cdot (273.16 - Ts)}{\rho w \cdot Lf} \quad (1)$$

Where:

CC- cold content, [mm]

ρ_s - snow density [kg m^{-3}]

c - specific heat of ice [J kg^{-1} K^{-1}]

d – snowpack depth [m]

Ts – average temperature of snow [K]

ρ_w – density of liquid water [10^3 kg m^{-3}]

Lf - latent heat of fusion [J kg^{-1}]

Cold content is more of a conceptual measure to describe the internal energy of the snowpack (Mosier et al., 2016). Jennings et al. (2018) in their review gives three basic estimations used to determine the C_C of the snowpack. The first one is a function of air temperature described in Allard. (1957). Second is a function of precipitation and air temperature (Cherkauer et al., 2003). The last method describes C_C as a residual of the snowpack energy balance used in Andreadis et al. (2009). Temperature-based index models generally employ the first mentioned method while physics-based models usually utilize the other two methods (Jennings et al., 2018).

While cold content has been shown to improve melt timing predictions (Mosier et al., 2016), few studies have been conducted on the factors driving cold content development. A study carried out in the Colorado Rocky Mountains by Jennings & Molotch. (2020) suggests that air temperatures had a small relation to the snowpack cold content. Snowfall, in contrast, contributed significantly to C_C development (more

in alpine than in subalpine snow pits). Further, negative energy fluxes were not as significant in contributing to the C_C as snowfall. This leads C_C to lower in days without precipitation and increase during days of snow accumulation.

However, especially in sub-alpine regions, C_C is affected by energy fluxes such as shortwave and longwave radiation and latent heat fluxes. In warming climate conditions, the C_C is expected to decrease, making snow more prone to melting with lower energy input (Jennings & Molotch, 2020). Another observation showed that peaks of C_C, precipitation and peak SWE could accurately help to predict snowmelt timing (Jennings et al., 2018).

2.2.2 Liquid water content and water holding capacity.

After the snowpack reaches the isothermal temperature of 0 °C, snow meltwater is still held in the snowpack until the liquid water holding capacity is exceeded (DeWalle & Rango, 2008). Liquid water holding capacity is the amount of water that can be held up against the gravity by capillary forces in the porous snowpack (DeWalle & Rango, 2008). In practice, the holding capacity is typicaly around 10% of SWE (Seibert et al., 2015b). The remaining liquid water will percolate through the snowpack and eventually reaches the soil, where it either forms basal runoff or infiltrates the soil (DeWalle & Rango, 2008). The sum of the water held against the gravity and water percolating through the snowpack is referred to as liquid water content (LWC). LWC can then be expressed in either volumetric unit or as a mass unit (kg or m^3). Both metrics are based on the rate of liquid water to the amount of snow (Fierz et al., 2009). The liquid water content is an important measure as it determines how much water is going to be released by melting. (DeWalle & Rango, 2008).

The liquid water content of snow also influences the snow avalanche formation (Hirashima et al., 2010), surface albedo (Dietz et al., 2012) and snow melt runoff timing (Hirashima et al., 2010; Avanzi et al., 2015). The role of LWC in ROS events has been demonstrated by Würzer et al. (2016). Where snowpacks with high LWC were observed more prone to generate high runoff by a piston flow mechanism described in Juras et al. (2016). Although, LWC can tell us a lot about the snowpack, its usage in research is relatively limited, mainly due to challenges associated with accurately measuring LWC (Lu, 2012). Existing studies have therefore focused on comparison of possible methods of LWC measurements (Fierz et al., 2009)

2.2.3 Energy balance

The processes of metamorphism or snow melt are dependent upon the snowpack energy balance, which describes the exchange of energy between the snowpack, the atmosphere, and the soil (Seibert et al., 2015b) (Fig. 2). The most significant elements of the energy balance of the snowpack are net longwave and shortwave radiation, convective latent heat, and sensible heat (together sometimes referred to as turbulent heat fluxes). Further, fluxes between soil and snow, and energy supplied by liquid precipitation, are considered despite their relatively minor contribution to the total energy balance (DeWalle & Rango, 2008). Most of the exchange is happening on the snow surface (DeWalle & Rango, 2008). The fluxes are then described as a sum of all components, where the fluxes entering the snowpack are considered as positive, while fluxes leaving the snowpack are considered as negative (Seibert et al., 2015b). Importance and fluctuations of the energy balance components are dependent on topography, local climate, vegetation, and weather conditions as well as the time of the day (Hotovy & Jenicek, 2020). The energy balance can be then described as in (Equation 2):

$$Q_m = Q_{ns} + Q_{nl} + Q_h + Q_e + Q_p + Q_q + Q_i \quad (2)$$

Q_{ns} = net shortwave radiant energy exchange (≥0)

Q_{nl} = net longwave radiant energy exchange (±)

Q_h = convective exchange of sensible heat with the atmosphere (±)

Q_e = convective exchange of latent heat of vaporization and sublimation with the atmosphere (±)

Q_r = rainfall sensible and latent heat (≥0)

Q_g = ground heat conduction (±)

Q_m = loss of latent heat of fusion due to meltwater leaving the snowpack (≤0)

Q_i = change in snowpack internal sensible and latent heat storage (±)

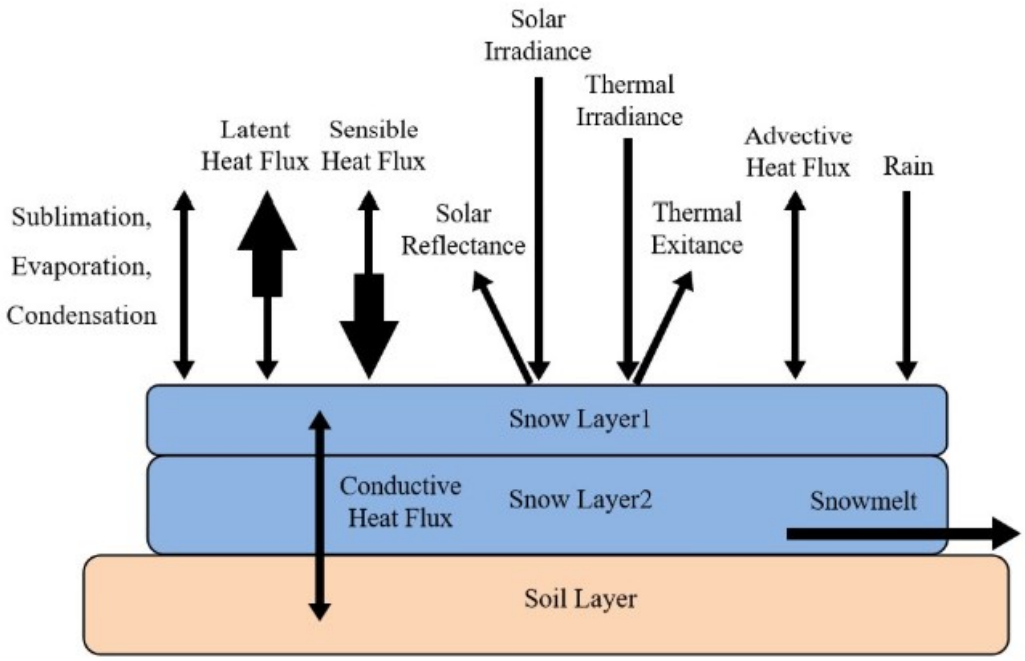

Figure 2: Schematic diagram of energy exchange between snowpack and the environment (Zhou et al., 2021)

The energy budget represents a physics-based method for modeling snow accumulation and melting. In research, a wide range of approximations is being applied and different models might be employed (Lackner et al., 2022). Since measurement of all fluxes can be challenging in the field conditions (Seibert et al., 2015b), alternative temperature-index approaches are often used to substitute for energy balance (Rango & Martinec, 1995; Jeníček et al., 2017;Ismail et al., 2023). A number have been conducted using enhanced degree-day model. For example, Hock. (1999) added direct solar radiation in clear sky conditions. Pellicciotti et al. (2005) used temperature-based model enhanced for LW radiation to model glacier melting and Ismail et al. (2023) was quantifying a physic-based factors such as snow albedo and cloud cover into a degreed-day factor. Limitation of a degree-day approach is that although it is effective proxy on longer time periods its accuracy decreases with shorter time steps, particularly in sub-day time steps (Hock, 1999). There for the degree-day method is the most effective for periods exceeding 10days (Hock, 1999).

In a scale of one day, meteorological events such as liquid precipitation can alter the significance of different heat and radiant fluxes (Garvelmann et al., 2014; Li et al., 2019). In study conducted by Würzer et al. (2016) it was shown that cloudy conditions, during rain-on-snow events (ROS) resulted in increase of longwave radiation as well as turbulent heat exchange. Studies done at Ptačí brook in Šumava Mountains, by Hotovy & Jenicek. (2020) showed that energy required for melting was predominantly supplied from longwave radiation for the snowpack located under a forest canopy. Further, the work suggests that while significance of ROS events might be negligible for

long time periods, in a day-scale energy balance, ROS can represent up to 29% of the energy budget (Hotovy & Jenicek, 2020).

2.3 Rain-on-snow

The term rain-on-snow (ROS) is used to describe a situation where liquid rain falls on a frozen snowpack (DeWalle & Rango, 2008). Such events are often referred to in the context of flooding, landslides, wet avalanche formations, slush flows and other geo-hazards (Brandt et al., 2022; Juras et al., 2017). This phenomenon is caused by the potential of incoming liquid rain to rapidly release a large amount of water from the snowpack that is higher than the initial rainfall amount, as well as its ability to change the snowpack stability (Juras et al., 2017).

ROS events have profound, costly and sometimes fatal consequences on human lives. A good example could be a flood in Canadian Alberta, where a large flooding in 2013 caused an evacuation of thousands of inhabitants and cost millions of dollars (Pomeroy et al., 2016). Due to these effects and costs of rain-on-snow, the phenomena is in particular focus of the hydrological community and even have been added to the twenty tree unsolved problems in hydrology (Blöschl et al., 2019). Further, projections of future climate in temperate regions predict that the frequency of ROS is going to increase as a result of rising air temperatures at higher elevations (Surfleet & Tullos, 2013).

The substantial amount of runoff generated by a ROS event is a bulk of rainwater and meltwater released by the snowpack. Snow melt can contribute about half of the subsequent runoff as reported in a study done at the Main River watershed by Sui et al. (2010), where snow melt contributed from 24% up to 64% of the exceptional run-off. Similar results were published by Wayand et al. (2015). Further, snow melt was reported to accompany 84% of ROS events, that generated excess snowpack runoff in the Swiss Alps (Würzer et al., 2016).

2.3.1 The energy fluxes during ROS

The energy contribution to the melting differs and usually only a small amount of energy is supplied by the warm rainwater (Hotovy & Jenicek, 2020). In studies done by Garvelmann et al. (2014) and Würzer et al. (2016) authors suggest that the main energy flux came from long-wave radiation, induced by cloud coverage and turbulent heat exchange. The share of these fluxes also varies with local meteorological conditions. Garvelmann et al. (2014) reported that during ROS events, snow melt on open sites was mostly induced by the turbulent heat exchange whereas in forest covered sites, the long wave radiation and turbulent fluxes held a same share. Similar results were observed at forest sites in Czech Šumava in Hotovy & Jenicek. (2020) or by Li et al. (2019) in USA where the main contribution in western USA was net radiation, but in eastern USA both net radiation and turbulent heat flux contributed equally.

2.3.2 Snowpack runoff during a ROS event

Although ROS events are associated with increased runoff, only a handful of ROS events result in an increased or very high runoff. The snowpack can hold up a considerable amount of water (Seibert et al., 2015b), thus it often acts like a barrier reducing, or even preventing runoff completely. A study conducted in north-west USA reports half of the largest ROS events did not lead to flooding (Wayand et al., 2015).Additionally, Kattelmann et al. (1987b) reported that forest covered catchment did not generate any additional runoff in response to ROS events. Snow therefore plays an ambiguous role in runoff generation. On one hand snowpack can release additional water in addition to the rain and on the other, it can mitigate or even prevent runoff completely. Additionally, snow cover commonly creates a time lag, between rainfall and the termination of water in the catchment. (Würzer et al., 2016; Wayand et al., 2015).

The quantity of released water is typically contingent upon the snowpack characteristics such as cold content, initial liquid water content, snow depth and spatial extent of prior snowpack as well as meteorological conditions such as temperature and intensity of the rain (Würzer et al., 2016). Snowpacks with low cold content or isothermal snowpacks tend to generate higher runoff in proportion to initial rainfall as the energy is used to melting rather than warming of the snowpack by refreezing (Beria et al., 2018; Juras et al., 2021). The variables of the snowpack affecting the snowpack response to ROS were extensively studied by Juras et al. (2021) where authors identified the main preconditions affecting snow response to ROS events. The combination of shallow snowpacks in with high rain volumes was likely to generate high runoff. Conversely, deep and extended snowpacks exposed to rain under cold temperatures were likely to generate moderate runoff and, in some cases, no runoff at all. A study conducted by Würzer et al. (2016) in the Swiss Alps concluded that the highest excess runoffs from a snowpack were generated within a short time after the rainfall, by a snowpack with high liquid water content. Wet snowpack can start to release liquid water stored in snowpacks pores (i.e. liquid water content) as incoming rainwater pushes it out. This effect can be described as a piston flow mechanism (Juras et al., 2016). Piston flow causes the water stored in the snow prior to the rain fall to leave the snowpack with subsequent release of meltwater. The received rainwater would then leave the snowpack last (Klaus & McDonnell, 2013). This effect has an impact especially for isotope hydrograph separation as rainwater and water stored in the snowpack have different isotopic compositions and mixing is not occurring (Klaus & McDonnell, 2013).

2.4 Effects of the forest canopy

It is established that forest cover has an impact on the snow accumulation, ablation and melting of snow as well as on its physical properties. Thus, the volume and ripeness of the snowpack in forest sites and open areas differs significantly. The forest presence, composition and stage therefore hold a key role in the snowpack ripening process, timing and the amount of runoff generated by snow in forested catchments (Hotovy & Jenicek, 2020). Disturbances and changes in forest canopy composition have caused a major difference in runoff timing and intensity (Bartík et al., 2019; Langhammer et al., 2015). Understanding the effects that forest canopy has on snow melt is there for important to accurately estimate water storage and flood modeling (Hock, 2003).

Open sites have been shown in many studies to accumulate on average up to 40% more snow than forested sites (Varhola et al., 2010). This is due to the tree effects of the forest cover. A) the tree canopy intercepts up to 60% of the snowfall. B) Three shading causes the change in incoming radiation (Hotovy & Jenicek, 2020) C) Forest prevents wind transport of snow, altering the redistribution of snow volume. (Varhola et al., 2010; Essery et al., 2003). These processes are rather complicated to model as they contain variables such as forest cover interception peculiarities or the large amount of data necessary that are difficult to measure (Hotovy & Jenicek, 2020).

2.4.1 Snow accumulation and distribution

Generally, accumulation under the tree canopy is lower as the snowfall gets intercepted and subsequently sublimated back into the atmosphere or melt (Essery et al., 2003). However, the relationship between the number of trees and snow accumulation is not linear. The three branches can intercept a certain amount of snowfall (Varhola et al., 2010). A study done in Idaho by Connaughton. (1933b) revealed that during small or mild snowfall years, forested sites accumulated 27.5% less snow than open sites. Yet, in average precipitation year, the difference between open and forested sites was only 4.3%. Similar results were obtained by Jost et al. (2007). The forest composition also plays a crucial role in peak snow accumulation. Deciduous forests generally accumulate more snow than coniferous forests. Winter effective leaf area index (LAI) seems to have a significant role as shown in Pomeroy et al. (2002) where low LAI sites like deciduous sites had a similar accumulation to open sites.

Clear cuts and meadows also alter the snow distribution by acting as a wind barrier. Snow accumulations are known to peak as the wind reaches the tree barrier and snow falls out of suspension. Many observations were made of snow average accumulation peaking in meadows or clearcuts in diameter smaller than three times the heigh of surrounding trees. Conversely, large areas show smaller accumulation than adjacent forests, as they are affected by wind transportation (Swanson,1988; Gelfan et al., 2004). Further, forest density plays an important role as it was observed by Veatch et al. (2009), where the highest accumulation was found in forest with canopy density

reaching from 25 to 40%. Snow depth in these sites was larger than the one observed either in open sites or densely forested sites.

2.4.2 Forest canopy Effect on snow energy balance

The forest composition is also crucial to the snowpack energy balance since the differences in energy fluxes between open areas and forests cause different snowmelt rates (Hotovy & Jenicek, 2020). Canopy shading from shortwave radiation (SWR) can lead to a longer-lasting snow cover while longwave radiation (LWR) emitted by trees can cause the opposite effect (Lundquist et al., 2013;Gouttevin et al., 2015). Further, trees act like a barrier for the wind, reducing the effect of turbulent fluxes in the snowpack energy balance. The last important effect of forest cover on the energy balance is debris material such as sticks, needles etc. that accumulate on the snow surface, changing its albedo (Gouttevin et al., 2015). The forest canopy effect on energy balance is there for a complex issue with great importance for snowmelt modeling attracting attention of many researchers (Essery et al., 2003;Gouttevin et al., 2015;Gelfan et al., 2004; Veatch et al., 2009).

In the scale of a whole snow season, the SWR and LWR are predominant fluxes dictating the melt intensity (Gelfan et al., 2004; Varhola et al., 2010). The specific contributions of LWR and SWR in forest sites and open areas were studied by (Hotovy & Jenicek, 2020). This extensive study conducted in the Šumava mountains compared radiation balance between forest sites with different stages of the forest disturbance caused by the bark beetle (healthy and disturbed) and open area over a three-year period. The results showed that forest sites disposed 7% of the amount of SWR of the open areas. Further, the forest site had a higher positive contribution of net LWR than the open site, where the net LWR came out negative. Snowmelt intensity was however higher at open sites as the LWR on forest site could not put up for the SWR. The forest disturbed by mountain bark beetle showed a 50% increase in modeled snowmelt rate in the 3-year period. When put to comparison, snowmelt intensities for healthy forest, disturbed and open sites were 3,3 mm/day 5,9 mm/day and 13,9 mm/day respectively. The study therefore showed the importance of LWR in snow ablation, even in open sites, where the LWR balance is negative. The process of snow ablation variance in open and forested sites were further studied by Brooks, et al. (2014) using stable water isotopes and will be further discussed in following section.

2.4.3 Forest canopy effect on stable water isotopes

Snowpacks under a forest canopy tend to be isotopically enriched due to canopy interception and subsequent evaporation that causes kinetic fractionation (Beria et al., 2018). The amount of enrichment is relative to the time of snow residence in the forest canopy as well as the prior snowfall size (Claassen & Downey, 1995). However, not a

lot of work has been done to fully understand changes in snow isotope variance caused by forest canopy composition (Beria et al., 2018).

Authors of Biederman et al. (2014) were comparing a freshly exposed site due to Mountain pine beetle (MPB) and a healthy forest site in the US Rocky Mountains. The exposed site was expected to show a higher peak SWE than the forested site, but the SWEs showed equal values. Investigation of isotope composition has shown that at the MPB-affected site the snowpack was isotopically enriched similarly to the forest snowpack, showing signs of kinetic fractionation (sublimation). Authors conclude that the newly exposed snowpack received more direct sun radiation, thus the sublimation was enhanced and equal in mass lost to the sublimation of snow intercepted by the forest canopy. Isotope variation provided insight on the snow processes, that would be hard to detect by only snow volume monitoring (Beria et al., 2018).

2.5 Snowpack runoff and climate change

2.5.1 Less snow, earlier snowmelt

Snow is one of the most rapidly changing hydrosphere components due to climate change (Musselman et al., 2017). Because of the tight connection between air temperature and the precipitation phase, more precipitation is expected to fall in the form of rain instead of snow (Jenicek, Seibert, et al., 2018; Ishida et al., 2019). Rising air temperatures have historically reduced snowpack volume and persistence as they cause later snow accumulation and earlier snowmelt (Musselman et al., 2017). For example, a study focusing on snowpack change done in the western USA by Zeng et al. (2018) has shown that the mean peak SWE in the most affected catchments decreased on average by 41% between the years 1982 and 2016. Moreover, most of the hydrological projections of the climate change impact conclude that peak snowpack runoff would shift 30-40 days towards winter, in Europe and the USA (Stewart et al., 2004; Zeng et al., 2018). In line with these findings, simulations for Czech mountain catchments project a decrease in peak SWE by 30% to 70% by the end of the 21st century. Furthermore, snowmelt season was shown to occur 3-4 weeks earlier in winter. The overall decrease in snow accumulation will affect soil and groundwater storage. Since the snowpack acts like a water storage, the decrease in winter snowpack could be associated with decreasing summer low-flows in rivers (Morán-Tejeda et al., 2013; Jenicek et al., 2021). With climate change, the effect of snowmelt water sourcing catchments runoff might decrease in higher elevations and even completely disappear in lower elevations.

2.5.2 The variety of snow accumulation

Snow drought can be caused either by high air temperatures or low precipitation, or a combination of both factors (Jenicek et al., 2021). On a global scale, the most controlling factor is the air temperature near the earth's surface. Temperature increase then has the largest impact in regions where winter temperatures are already close to zero

(Thackeray et al., 2019). A similar impact could be observed in times of year like fall or spring as the temperatures are also close to zero (Thackeray et al., 2019). Therefore, mid-latitude snow cover appeared to be the most sensitive to climate warming with an approximate loss of $1.9 \times 106 km^2$ of snow per every Celsius degree temperature increase outside the tropics (Mudryk et al., 2017; Thackeray et al., 2019). Climate projections suggest conspicuous changes in precipitation patterns, with unresolved outcomes for central Europe as both increased and decreased precipitation could be expected. Further, an increase in precipitation might occur in winter while summer precipitation is expected to decrease. This increased winter precipitation is likely to fall out in the form of rain rather than snow fall. (Thackeray et al., 2019).

In snow accumulation changes, elevation plays a key role as air temperature change becomes less important above a certain threshold elevation, and precipitation becomes the predominant aspect of snow accumulation (Jenicek, Seibert, et al., 2018). In a study Marty et al. (2017) of catchments in Switzerland, it has been shown that snow accumulation might decrease by 50% at elevations higher than 3000m a.s.l. and almost no snow cover might form under elevations lower than 1200m a.s.l. by the end of the 21st century. Similar results were obtained by Morán-Tejeda et al. (2013), where the authors determined that snow accumulation is mainly influenced by air temperatures up to 1500 m ± 120 above average sea level. Above this threshold line, precipitation is the determining factor of snow accumulation. With rising temperatures, this line is expected to climb up.

Hydrological responses to climate changes are particularly complex as they can show more variance, compared to input climate projections (Jenicek et al., 2021). For central Europe, climate models often disagree in projections of the future changes in precipitation (Svoboda et al., 2016). This is particularly important as the increase in total precipitation could buffer the impacts of decreasing SWE (Marshall et al., 2020; Jenicek et al., 2021). In a study done in the western United States by Marshall et al. (2020) the authors suggest that the increased snowfall intensities could probably buffer the decrease in snowpack in the continental parts of the USA. In contrast, maritime regions will suffer from the decreased snowpack as precipitation is expected to decrease. An indication of a similar effect was found in Czech mountain catchments. Jenicek et al. (2021) suggest decreased in snowfall might be partially compensated by the increased liquid precipitation in the winter.

3 Material and methods

3.1 Study area description

The research was conducted at an experimental site of Charles University within a Ptačí brook catchment, which is part of the Vydra river system. The site is situated in bohemian forest (Šumava National Park) on the border between Czechia and Germany. Data was collected from snow pits located in forest plot and open plot (Fig.5). Both plots are positioned in a flat terrain of approximate elevation of 1140m a.s.l. Over the winter of 2024 four field measurements were carried out with intervals of roughly 3 weeks (February-March). The Ptačí brook catchment is an experimental area managed by Charles University, offering a well monitored environment for hydrological or environmental research.

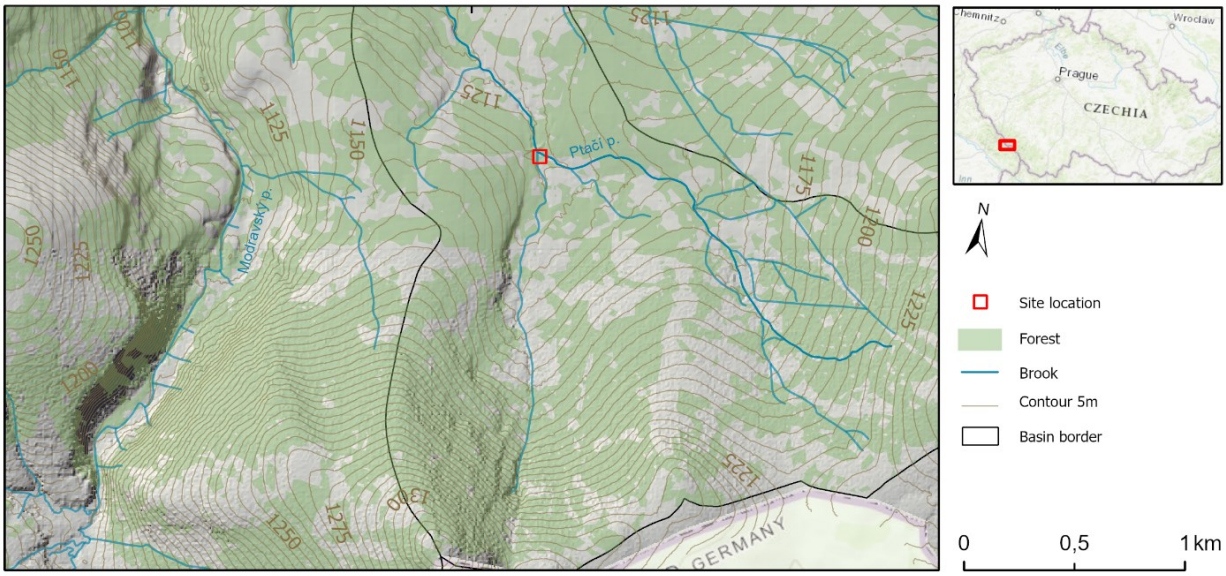

Figure 3: Geographical Location of the study area (DIBAVOD, ZABAGED®, Corine-landcover)

The catchment has an average elevation of 1201 m a.s.l. characterized by predominantly gentle, low slope terrain. Approximately 70% of the area features slopes of less than 7°, while half of the area has slopes under 5°. This flat terrain is particularly evident in north-eastern regions of the watershed, where the snow pits site is located. In contrast, the south and eastern part exhibits more indented terrain.

3.1.1 Climatic conditions

The study area is strongly influenced by the south-westerly wind flow, which is reinforced by the orographic effect of the windward side of the Šumava mountains. As a result, the area is one of the most precipitation-rich locations in Czechia. The amount of precipitation in the wettest summer month (June) is approximately (120 mm). According to the time series (1961-2023) the driest months are October and April. The average air temperature of the warmest month does not exceed 22°C, while only 1-2 months usually reach an average air temperature higher than 10°C. The average

annual precipitation at Filippova Huť station is 1200 mm. At the study site, the average annual temperature is 4°C and -2 to -5°C during the cold season (Hotovy & Jenicek, 2020). The mean precipitation in the cold season (November -April) is about 400 mm, most of which falls as snow. Snow accumulation typically begins in November and snow cover lasts until March or mid-May, while snowmelt runoff typically represents about 30-40% of catchment runoff (Hotovy & Jenicek, 2020). Mean snow depths are generally higher than 80cm from December to April.

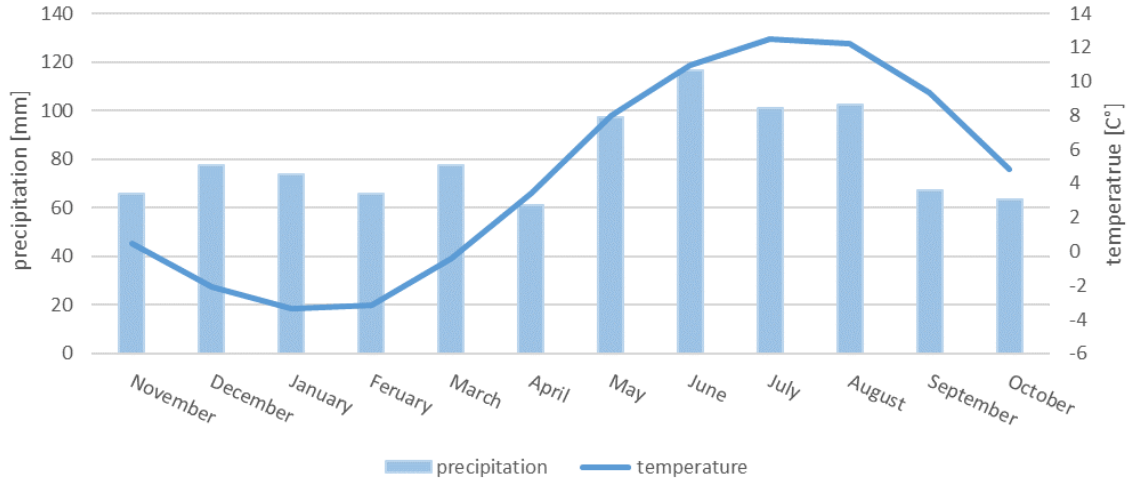

Figure 4: Annual cycle of average air temperature and precipitation sums at Churáňov Station (data: ČHMU)

3.1.2 Site description

The forest cover of the catchment is mainly formed by Norway Spruce (Picea abies) dominated coniferous forest. Forests in the area have undergone a vast disturbance caused by the Bark beetle (*Ips typographus*). Forest cover is therefore variant, formed by healthy forests, disturbed areas with dead trees as well as regenerating areas with young vegetation. The changing forest cover affects the snowpack as it alters wind redistribution and snowmelt (Hotovy & Jenicek, 2020). Therefore, the forest plot has been selected in a healthy forest with a connected forest canopy and rare floor vegetation. Forest snow pits were conducted far enough in the forest to prevent snow deposited from wind redistribution to affect the snow profiles.

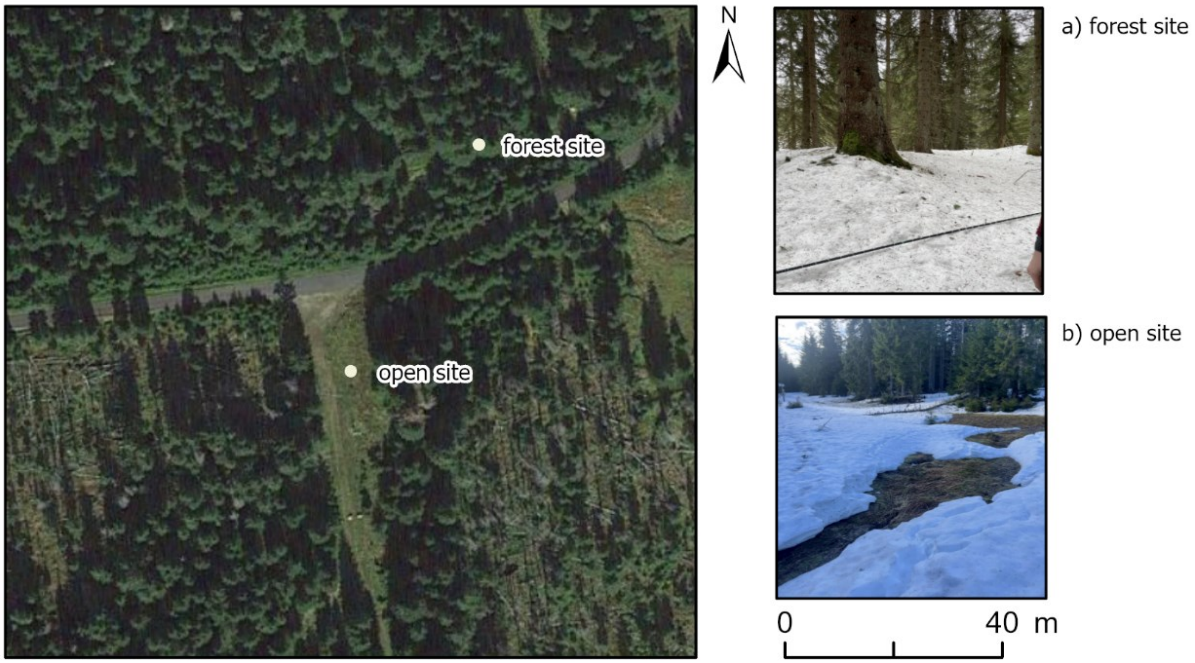

Figure 5: Location of forest site and open site (orthophoto ČUZK, authors photography)

The open site as depicted in (Fig. 5) is a small opening of diameter approximately 15m. Surrounding trees do not cause a significant shading of direct radiation. Since the area is relatively small, surrounding trees prevent wind redistribution that could otherwise cause inconsistency in the snow stratigraphy data. The slope in both plots is negligible, preventing the occurrence of a major lateral flow of water within the snowpack. The approximate elevation of both plots is 1132 m a.s.l.

3.2 Methods

3.2.1 Theory of stable water isotopes in snowpack

Isotopes are variants of the same atom, differentiating by the number of neutrons in their nuclei. Stable water isotopes are often used as a natural tracer for hydrograph separation (Klaus & McDonnell, 2013). In natural form, hydrogen exists in two forms (^{1}H and ^{2}H also referred to as deuterium). Oxygen then exists in three forms (^{16}O, ^{17}O, ^{18}O). The isotopes referred to as lighter or depleted in heavier isotopes such as ^{2}H or ^{16}O are more common in nature with relative occurrence of 99,76% for ^{2}H and 99,98% for ^{16}O (Sharp, 2017). The isotope values in samples are expressed as the ratio R of the concentrations $^{2}H/^{1}H$ or $^{18}O/^{16}O$. These ratios are standardized to the Vianna Standard Mean Ocean Water (VSMOW2) (Beria et al., 2018), which is a standard ratio of water isotopes defined for the ocean. VSMOW2 then acts as a benchmark to which the isotopic composition is compared to either as enriched or depleted in heavier isotopes. The δ ratio is then given in (‰) calculated by Equation 3:

$$\delta 18O \; or \; \delta 2H = \left(\frac{Rsample - Rvsmow}{Rvsmow}\right) \cdot 1000 \tag{3}$$

Where R_{sample} is the isotopic ratio of the water and R_{vsmow} is the ratio of the Vienna standard. If the δ is greater than 0, the sample is referred to as enriched in comparison to the Vianna standard. Similarly, if the δ is smaller than 0 the sample is depleted. As most precipitation originates from ocean evaporation, the meteorological water tends to show negative values of δ. This is caused by different chemical and physical properties caused by different masses of isotopes, which result in preferential sampling of different isotopes in phase changes e.g. fractionation. As a result, water has a unique isotopic composition, revealing the processes that it went through which allowing us to track its origin (Beria et al., 2018).

There are two types of fractionations, namely equilibrium and kinetic fractionations. A typical example of equilibrium fractionation is condensation. Condensation is a process of equilibrium fractionation where the condensate ends up enriched in the heavier isotopes compared to the remaining water vapor with the similar ratio of $\delta^{18}O$ and $\delta^{2}H$. An example of the kinetic (non-equilibrium) process is evaporation, where the vapor ends up being isotopically depleted in heavier isotopes, which remain in the liquid phase. In contrast to equilibrium fractionation, the phase change effect of evaporation is stronger for changes in $\delta^{2}H$ compared to $\delta^{18}O$, resulting differential enrichment in $\delta^{2}H$ and $\delta^{18}O$ in the remaining phase (liquid). (Beria et al., 2018).

As the δ^{2} H and d $\delta^{18}O$ are part of the same molecule and both modified by mass dependent on the fractionation process, the relation of δ^{2} H and $\delta^{18}O$ is almost linear and can be described as a global meteoric water line (GMWL) (Craig, 1961) in Equation 4:

$$\delta 2\,H = 8 \cdot \delta 18O + 10 \tag{4}$$

The interception of GMWL is referred to as *d-excess* (deuterium-excess factor) and is used to distinguish between equilibrium and nonequilibrium processes (Beria et al., 2018; Galewsky et al., 2016). However, the GMWL is a product of samples originating from locations all around the world, therefore they might not be representative in a specific locality, depending on the source of precipitation water. Local meteoric waterline (LMWL) is used to describe the relationship of δ^{2} H and $\delta^{18}O$ at a given site. Water samples that undergo equilibrium (e.g. condensation) fractionation processes are located along the LMWL, meanwhile, water undergoing non-equilibrium processes such as evaporation or sublimation, usually show higher values of $\delta^{18}O$ to $\delta^{2}H$ in the remaining phase (liquid or ice), thus resulting in a different slope of the line as shown in (Fig.6).

Backtracking the local evaporation line provides an estimate of the initial isotope ratio (Beria et al., 2018;Rose, 2003).

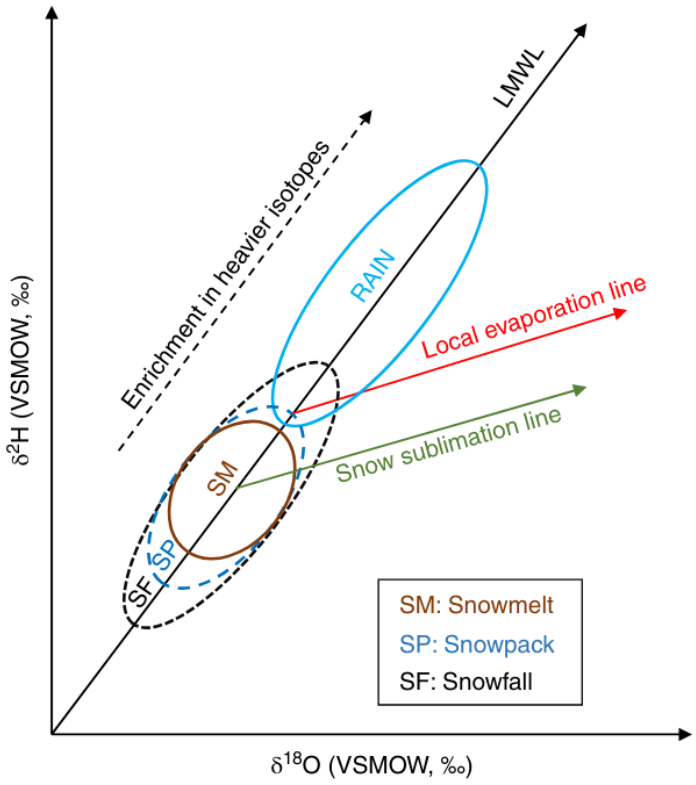

Figure 6: Conceptual representation of possible sample positions in the dual isotope space (formed by δ^2H and $\delta^{18}O$) for snow and rainfall samples from an entire hydrological year (Beria et al., 2018).

The isotopic ratio is largely determined by the temperature of condensation or cloud condensation temperature. The higher the temperature, the more is the precipitation enriched in heavy isotopes (Beria et al., 2018; Dody et al., 2013). Another factor affecting the isotope ratio is the distance that the molecule travels in an air mass, as with greater distance from the ocean, precipitation becomes more depleted in heavier isotopes (Valdhasova, 2020;Cane & Clark, 1999). Another effect can be observed during rain, where at the beginning the heavier isotopes fallout from the cloud as rain or snow leading the precipitation to become continually more depleted in heavier isotopes. This effect is referred to as *rain-out-effect* (Beria et al., 2018; Schürch et al., 2003). A similar scenario can be observed with elevation gradients where precipitation falling out at lower elevations tends to be more enriched in heavier isotopes than precipitation at higher elevations (Beria et al., 2018).

3.2.2 Snow pits and snow properties measurements

In the winter season of 2024 together four trips have been made over the span of three months. These measurements were conducted on 22 February, 1 January, 16 January and 1 March. Snow samples for δ^2H and $\delta^{18}O$ analysis were collected from each identified layer of a snow pit and set in bottles of 50ml that were kept in a fridge to prevent water evaporation. These samples were later analyzed at the Institute for Hydrodynamics of the Czech Academy of Sciences using PICCARO L2130-I laser spectrometer.

In addition, measurements of snow hardness, snow grain type, grain size, and snow profile temperature as well as snow water equivalent (SWE) for the whole profile and every identified layer were conducted. All measures followed the methodology of international classification for seasonal snow on the ground (ICSSG) (Fierz et al., 2009). These snow pit data were later visualized using niViz open-source software.

Snow density and SWE were measured with a cylinder of cross-sectional area of $50cm^2$ and a digital weight. The SWE was calculated as shown in (Equation 5):

$$SWE = 200 \cdot m \tag{5}$$

Where SWE is the snow water equivalent in mm and m is the mass of the snow. The mass is multiplied by 200 to determine the snow water equivalent for 1 m², given the area of the measuring cylinder is 50 cm². Using SWE, the density of each layer could then be calculated as described in (Equation 6)

$$SWE = \rho \cdot h \cdot 10 \tag{6}$$

Where SWE is the snow water equivalent in mm, ρ is the snow density in g/cm³, and h is the snow layer height in centimeters. The overall snow density was calculated as the weighted average of the densities of individual layers, weighted by the height of the layers.

3.2.3 Meteorological data

In addition, to field measurements, meteorological data are also available from meteorological stations in the catchment. At the Ptačí potok, a Snowpack Analyzer (SPA) and snow pillow are installed, measuring the snowpack SWE. The SPA device is then used to measure the depth, water content, density of the snow, and the content of the

liquid and solid phases within the snow cover (Jeníček et al., 2017). Further winter precipitation using a heated gauge is measured at the meteorological station in Modrava which is located roughly 5km from the study site. The incoming and reflected shortwave and longwave radiation is measured using a CNR4 Net. This device consists of two pyranometers (the first is oriented upward, and the second is oriented downward) and two pyrgeometers (with the same configuration as pyranometers). This configuration makes it possible to measure the global and reflected radiation for albedo calculation (Jeníček et al., 2017).

Data provided by these stations occasionally yield data indicating an error of measurement, these data were deleted and might appear missing in produced graphs. Timeseries and other graphs were produced using Microsoft Excel.

4 Results

4.1 Snow season in the Ptačí brook catchment

The winter season of 2023/2024 in the Šumava Mts. was relatively long but predominantly snow-poor, with few exceptions. Initial snowfall occurred in mid to late October, with snow depth remaining modest (around 20cm) through early November. The first significant snowfall was observed in late November forming the first substantial snowpack. An unusually high accumulation period came in late December, where the period of heavy snowfall set the highest snow depth for December since the start of monitoring (snow depths of 85cm). January snowpack showed a considerable fluctuation in snow depth and snow water equivalent, indicating changing atmospheric conditions that are displayed in (Fig.8) and (Fig.9). In January, periods of snow accumulation were often followed by rain and subsequent snowpack loss. The observed precipitation and thawing caused increased water levels and floodings in the region (Lipina,2024). Further, snow height decreased while SWE has shown a fluctuating nature, seemingly not reaching values below approximately 150mm until 16 February (Fig.8).

From March onward we observed a gradual decline of the snowpack. By early April, snow levels had diminished to approximately 40 cm. This reduction aligns with the onset of the melting period, typical of the seasonal transition from winter to spring.

During the monitored period, about two significant ROS events occurred (Fig.8). The ROS events align with peaking SWE and subsequent loss of SWE (found between measurements of 1 February and measurement of 16 February.

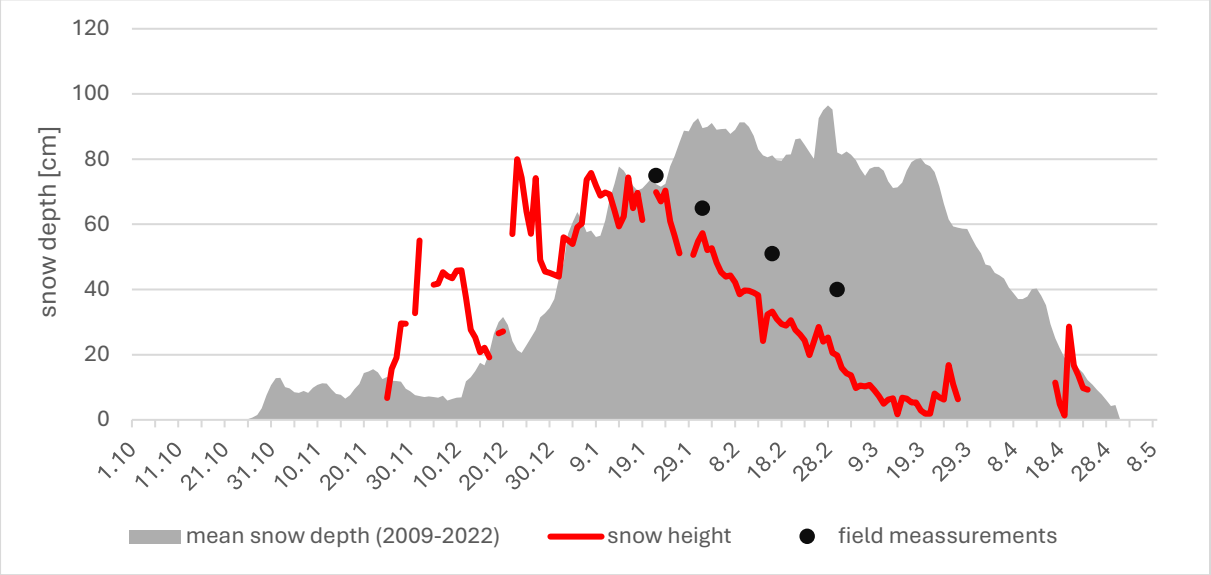

Figure 7: Snow depth measured at a climate station located in the Ptačí brook catchment in the winter season 2023/24 (red line) compared to 2009-2022 average (5 day moving average) snow depth (grey area) (data: KFGG).

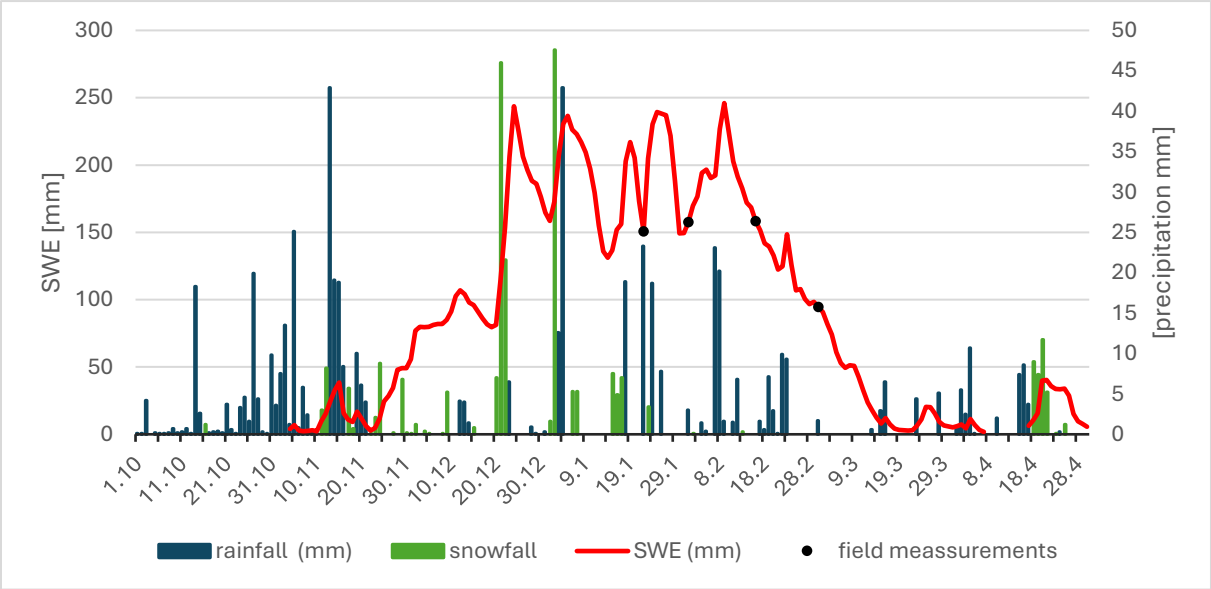

Figure 8: The SWE measured at the meteorological station at the study site. Precipitation events are measured at nearby Modrava station (5km). Depicted snowfall is precipitation occurring during periods at below 0 ºC air temperature at the study site. (data: KFGG)

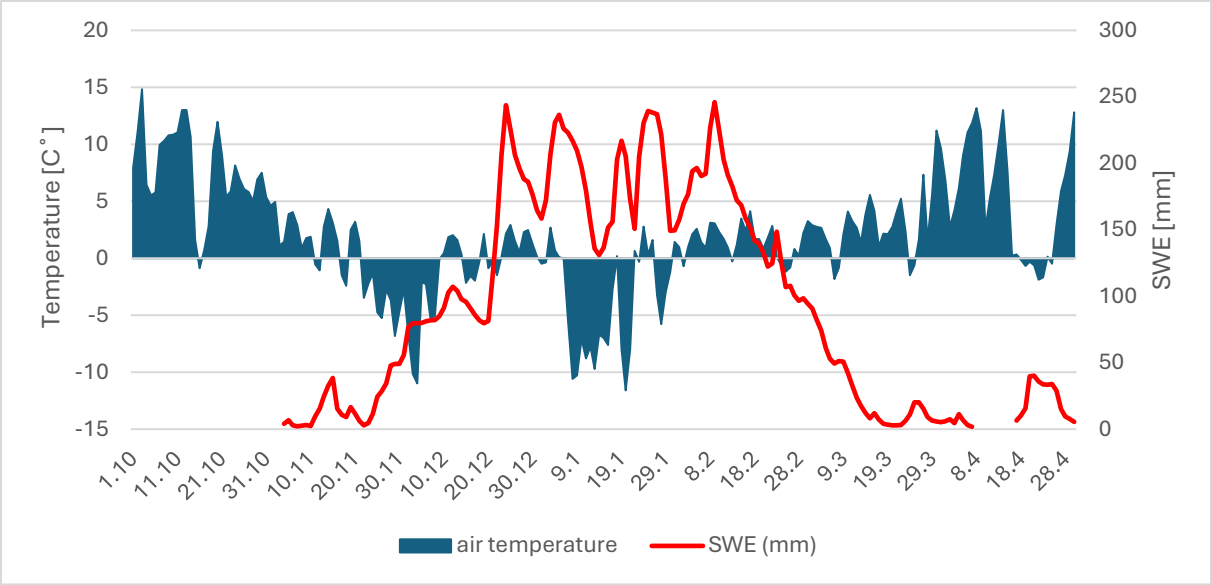

Figure 9: Air temperature measured by the meteorological station at the study site and SWE, measured by a snow pillow at the study site. (data: KFGG)

4.2 Spatial and temporal variability of snowpack characteristics

4.2.1 Snow depth and snow water equivalent variability

During the winter season of 2024, four measurements of physical properties (SWE, snow depth, snow hardness) were conducted in an open site and forest site. The open area exhibited higher values of snow depth and SWE. Snow depths in both the forest and open site were decreasing almost linearly during the spam of the measurements. The open area's initial snow depth was 75cm at the first measurement, later decreasing to 65cm 55cm, and 40cm for the 2nd 3rd, and 4th snow pit respectively. Physically measured snow depths were in equilibrium with data measured by the station (Fig.7). Local variabilities in snow depth may be caused by wind redistribution. A similar linear decrease in snow depth could be observed in forest snow pits where snow depths were 35cm, 31cm, and 15cm for the 1st, 2nd, and 3rd measurements respectively. In the forest site, all snowmelted by 1 March. Snow height data suggest an overall steady decline in snow depth with a similar rate for the forest and the open plot.

Different processes were observed in snow water equivalent, where while SWE at the forest site was steadily declining, the open area was showing a significant fluctuation in SWE (Fig.8). The values of SWE for forest site and open site measured by the station are shown in (Table 1). In this case, only physical measurement data was available for forest sites and therefore it is not clear whether SWE fluctuations appeared at the forest site as well as at the open site. Open site SWE data, physically measured during field trips, does not follow the data measured by the station (Table 1). The field measurements show proportionally higher SWE than the data acquired from the station. The

difference in values measured by the station and during field measurement could be due to a digital weight error or simply a mistake made during the measurement. However, field data follows a trend set by the station data, showing a small increase between 22 January and 16 March and decrease later. When comparing open area data from the station to field data from the forest plot, it appears that the forest showed a steady decline in SWE while the open area went through periods of accumulation and loss of SWE. This could be explained by shortwave radiation shading provided by trees, making the forest snowpack less responsive to SWR melting, and simultaneously by forest canopy interception of either snow or rain precipitation, preventing liquid water from reaching the snowpack. Since only a little snow precipitation was observed in the span of the measurements (Fig.8) the fluctuating SWE in the open plot could then be a result of frequent rains, increasing the SWE of a snow pit during the period of water residency in the snowpack.

date	SWE forest	SWE open (SPA)	SWE open area
22.1	114	150	194
1.2	94	157	312
16.2	60	158	214
1.3	0	94	210

Table 1: The development of SWE [mm] in open areas and forest areas, SPA represents the values measured by The SPA station.

4.2.2 The variability of snow stratigraphy

Using a magnifying glass, snow grain types and sizes were identified in each snow pit. SWE measurements were also carried out for each layer, enabling density estimation. Due to errors in measurements, some layers are missing density values.

Snow pits located in the open plot showed higher variability in snow grain sizes and types of metamorphism resulting in higher grain type variability. Whereas forest covered profiles were generally more homogenous indicating steady conditions, probably induced by the atmospheric shading of the forest. In both profiles, the highest variability of snow grain size was observed in the top layer of the snowpack representing the interface between snow and the atmosphere, as shown in (Table 2). Both the forest and the open area snowpack have shown a predominant presence of equi-temperature metamorphism (ETM) and wet-snow metamorphism.

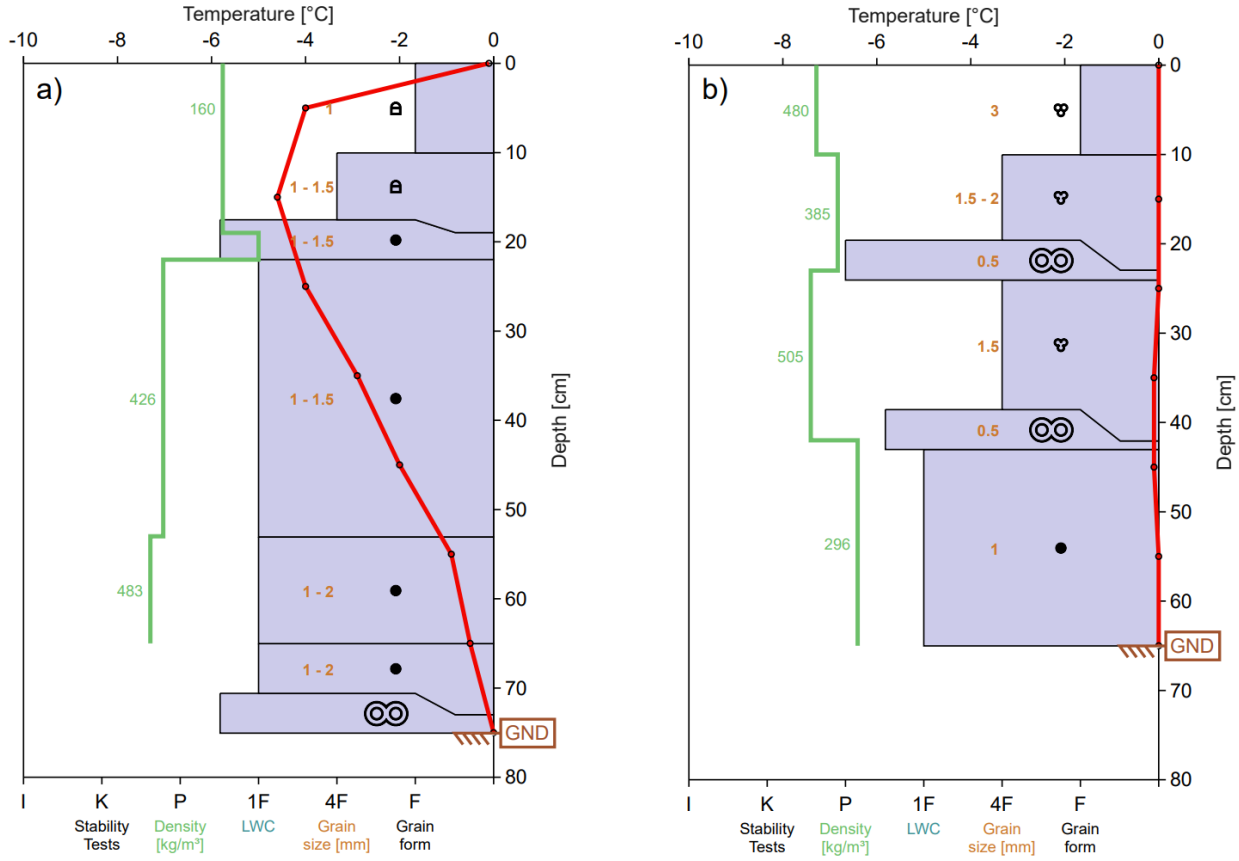

Figure 10: Open plot snow stratigraphy profiles on a) 22nd January, b) 1st February show the density (SWE) (green line) of every layer, temperature (red line), grain type, and snow hardness based on (ICSSG) (Fierz et al., 2009). The profiles were visualized using niViz software (niviz, 2023)

The first snow pit in the open area shown in (Fig.10a) showed significant stratification and a strong temperature gradient throughout the snowpack (although later in the season the snowpack turned to quasi-isothermal) reaching the lowest temperature of -4,6 ºC with 15cm snow depth while the temperature of the surface (depth 3cm) was -0,1 ºC. This strong temperature gradient between the upper layers indicates cold conditions preceding the field measurement visible in (Fig.9). Facet crystals, formed due to the strong gradient, were identified in the top layer. More homogenous layers can be observed between the snow depth of 25cm and the base. A small loss of density at 20cm might indicate an upward advection of water vapor caused by the gradient. The melt-freeze layer at the bottom suggests a positive energy flux from the underlying soil (the temperature of the soil was 0,8 ºC).

Snow profiles conducted from 1 February all showed a quasi-isothermal state with minimal deviation from 0 ºC occurring in the middle layers. The 2nd profile (Fig.10b) shows a melted form of snow present in upper layers and new melt-freeze layers in depths of 42cm and 23cm. These melt-freeze layers are possibly results of water originating from either snowmelt or ROS events refreezing in the lower layers of a snowpack.

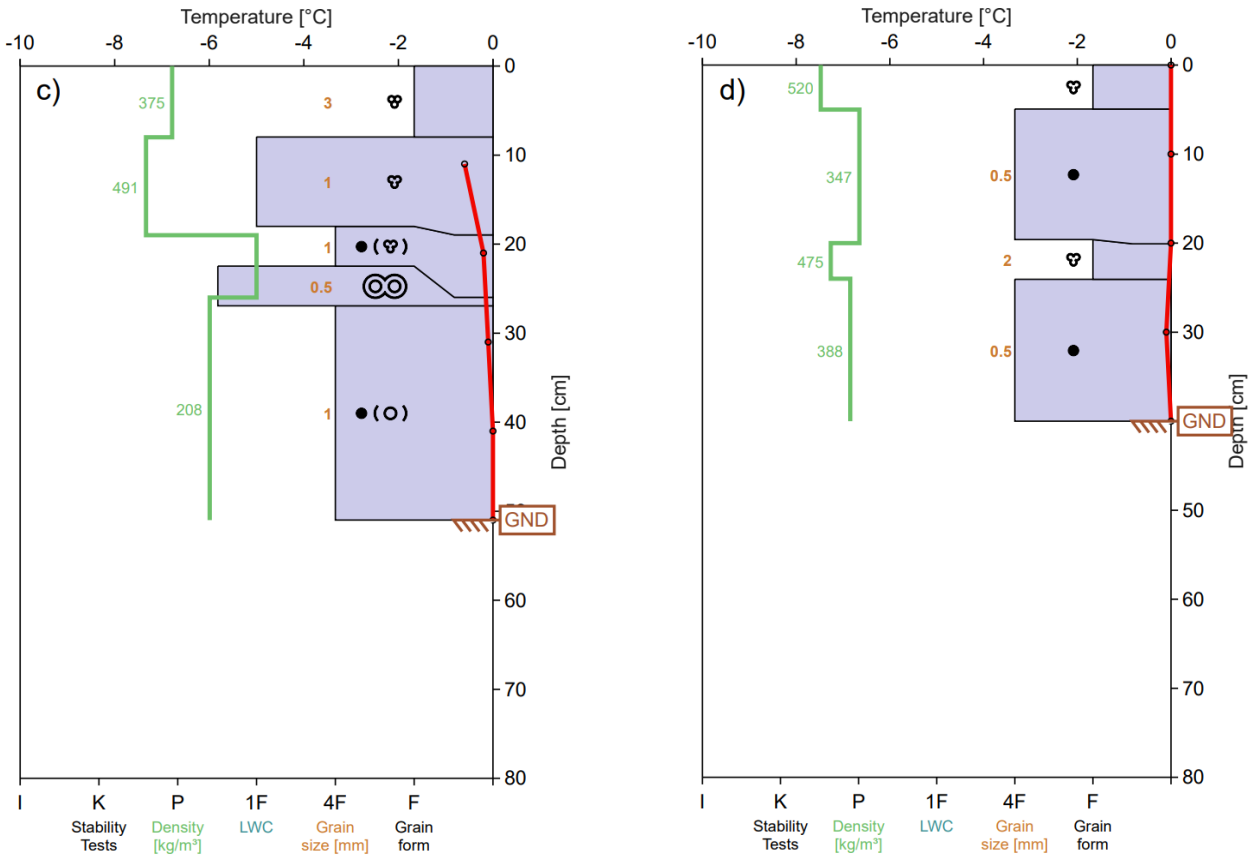

Figure 11: Open plot snow stratigraphy profiles on c) 16th February, and d) 1st March show the density (SWE) (green) of every layer, temperature (red), grain type, and snow hardness based on (ICSSG) (Fierz et al., 2009). The profiles were visualized using niViz software (niviz,2023).

On 16 February the profile exhibited a decrease in the upper layer while a stable rounded grain base layer persisted (Fig.11c). The melt-freeze layer was still intact in snow depth of 28 cm. From the snow profile on 1 March a similar trend of surface snow ablation was observed with a persistent base layer of rounded crystal at the bottom. Further, upper layers exhibited high densities (SWE) on 16 February and 1 March profiles indicating storage of melt and rainwater in those layers. Between the 3rd and 4th measurements snow height gain of 8cm was recorded by the station possibly resulting in the top layer of the last profile with lower hardness and higher density.

Forest stratigraphy profiles (Fig.12) were less diverse showing a maximum of 3 stratigraphic layers at snow height maximum, recorded on 22 January. Moreover, the 16 February profile only reached a snow depth of 15cm, with only two stratigraphic layers, therefore, only 22 January and 16 February snow pits are visualized in (Fig.12). All detailed structure profiles can be found in the appendices section.

The layers present on 22 January showed similar trends as layers in the open plot, with a stable, drier, rounded grain layer found at the bottom of the snowpack in both locations. Similarly, throughout the observed period, the upper layers showed signs of a high temperature gradient metamorphism later turning into wet snow melting layer. The absence of some layers in the forest snowpack compared to the open plot snowpack may therefore be caused by the interception of the forest canopy and subsequent melting of the intercepted snow before reaching the snowpack. Another observed difference in the forest snowpack was the on average higher temperature of the snowpack, with the lowest recorded values of -1,3 ºC on 22 January. Possibly due to the tree's emittance of LWR as well as the forest preventing other turbulent heat exchanges between the snowpack and atmosphere (Hotovy & Jenicek, 2020).

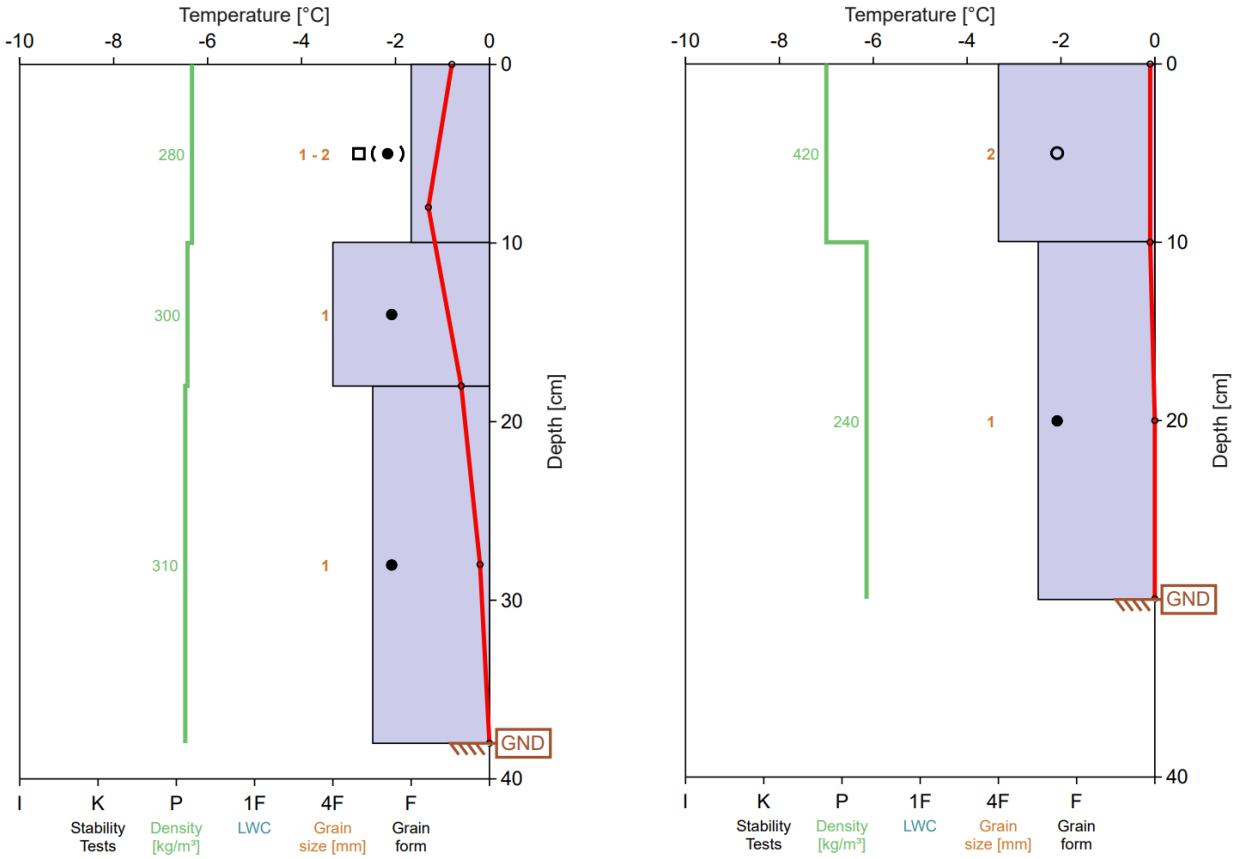

Figure 12: Forest plot snow stratigraphy profiles on 22th January (left) , and 1 February (right) show density (green) of every layer, temperature (red), grain type, and snow hardness based on (ICSSG) (Fierz et al., 2009). The profiles were visualized using niViz software (niviz, 2023).

4.2.3 Variability of stable water isotopes in snowpack

During the winter season of 2023/2024, together 26 samples of snow were analyzed. Additionally, precipitation and stream water were analyzed for stable water isotopes serving as a reference (Fig.12). The local meteoric water line (LMWL) was derived from measured precipitation values δ^2H and $\delta^{18}O$ (Fig.13). LMWL is then given:

$$\delta^2H = 7{,}59 \times \delta^{18}O + 4{,}8 \quad (7)$$

The LMWL closely follows the global meteoric water line (GMWL), which is indicated by the black line in Figure 13, suggesting that evaporation has not occurred during sample transportation and storage before the analysis. Local precipitation follows GMWL closely with slight deviation, possibly explained by local climatic influences. Additionally, precipitation is broadly spread along the LMWL showing high isotopic variance of local precipitation. Lower values of precipitation δ^2H and $\delta^{18}O$ could represent snowfall mixing in the precipitation collector while the higher values belong to rain precipitation. Snow samples from the forest plot seem to show a smaller variance in heavy isotope enrichment. These forest snow samples are located slightly to the right side of the LMWL and GMWL, possibly undergoing more evaporation or sublimation caused by the forest canopy interception. In contrast, stream water collected from Ptačí brook shows a little spread alongside the LMWL as the stream water is a mixture of all depicted sources. Further, the position of spring water values above both lines indicate minimal effect of evaporation.

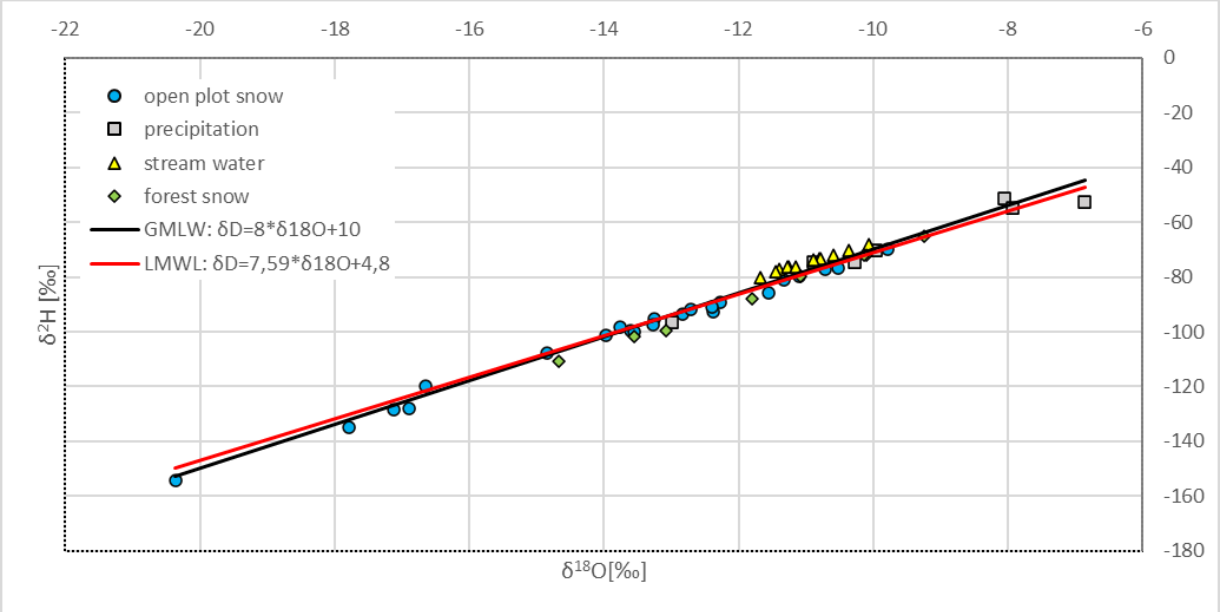

Figure 13: Isotopic composition of the snow, stream and precipitation samples collected in the season 2024. Black line represents global meteoric water line (GMWL), red line represents local meteoric water line (LMWL)

A total of seven samples were obtained from the snowpack under a forest canopy while 19 samples were collected from the open area. The forest samples exhibited stable, increased enrichment in heavier isotopes and decreased variability of $\delta^{18}O$ and $\delta^{2}H$ (Fig.14). The enrichment in heavier isotopes may be the result of the interception of precipitation by the forest canopy, where the snow is subject to sublimation before reaching the snowpack. Similarly, this may be attributed to the higher temperature of the forest snowpack, allowing for melting and outflow of the meltwater. The reduced variability of forest snowpack may also be result of a small number of identified layers (3 layers at recorded snow maximum).

The weighted average values of forest snowpack (weighted by identified layer thickness) were found to be $\delta^{18}O$=-12,64‰ and $\delta^{2}H$= -94,057‰ at the initial measurement conducted on 22 January. The isotopic values of the samples from 16 February, the final measurement before complete snowmelt of the forest snowpack, were $\delta^{18}O$=-10,09‰ and $\delta^{2}H$= -72,911‰. These results demonstrate a consistent depletion of lighter isotopes throughout the forest snow ripening process

In contrast, the open area showed higher variability in stable water isotopes (Fig.14), with a gradual depletion in lighter isotopes observed between 22 January and 16 February. A notable decline in variability was observed between 1 February to 16 February (Fig.14), which is likely due to a substantial ROS event that occurred 7-8 February, followed by an overall isotopic enrichment of the profile (Table 2).

The isotopically light layer at the base of the snow pit on 1 March, with values of δ18O = -20.37‰ and δ2H = -154.28‰, labelled as G in (Fig. 15a), increases the variability shown in the boxplot (Fig.14). This layer displays an unusual depletion in heavier isotopes in comparison to adjacent layers and layers in other profiles. A potential explanation for the sudden occurrence of this layer is the local topography of the open plot, where earlier snow accumulated in a local depression possibly due to wind redistribution. This likely resulted in the formation of an isotopically distinct layer not observed in other profiles. When considering only the adjacent layers of the 1 March snow profile, the trend indicates a continuous homogenization of the snowpack's isotopic values alongside a consistent depletion in heavier isotopes.

weighted average 18O/2H	22.January	1.February	16.February	1.March
open area δ18O	-13,489	-14,239	-12,06	-15,76
forest area δ18O	-12,647	-10,108	-10,094	
open area δ2H	-98,663	-104,69	-88,47	-117,04
forest area δ2H	-94,057	-72,061	-72,911	

Table 2: Weighted average of isotopes 18O and 2H for each snow pit on an open plot and forest plot.

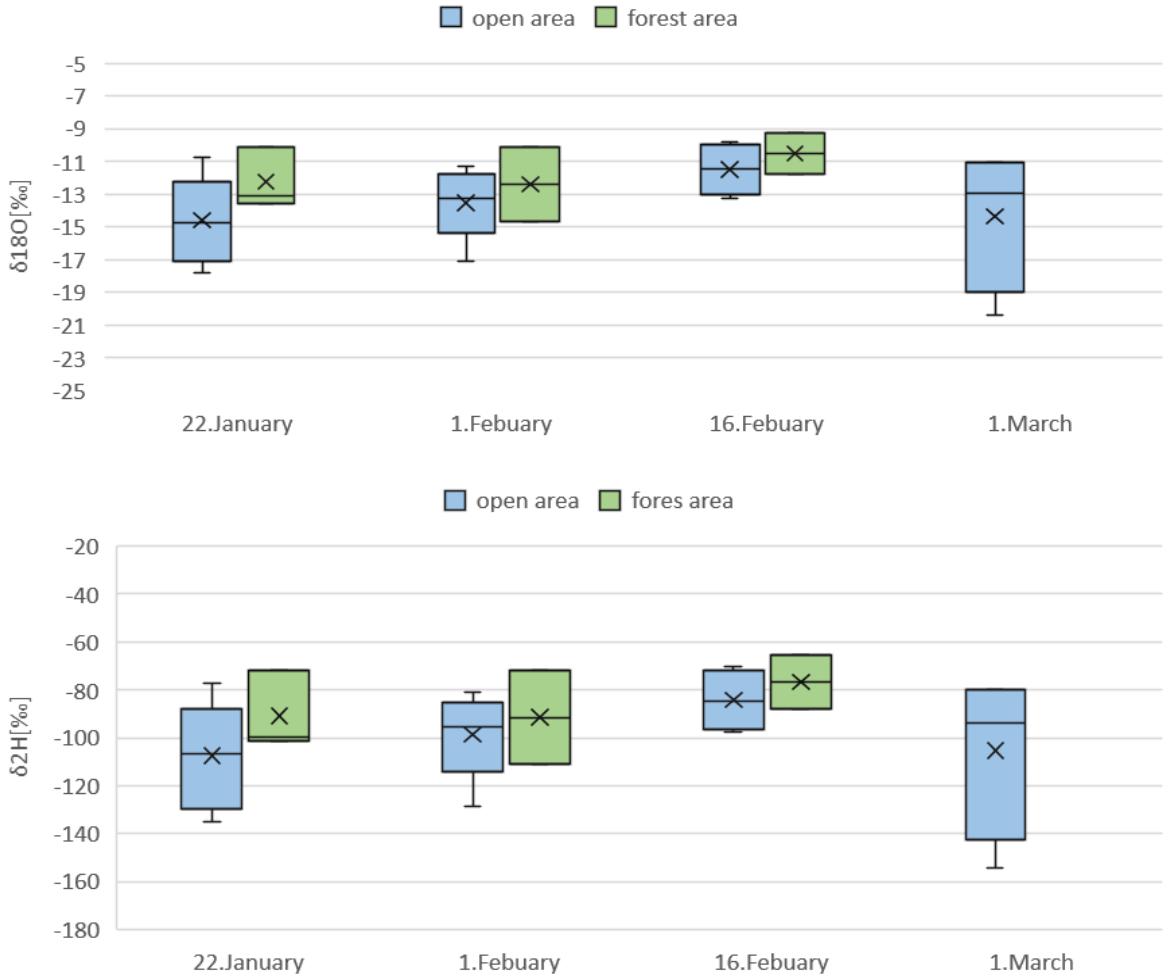

Figure 14: Box plot diagrams of the variability of isotope ratios δ2H and δ18O of snow cover for open area and forest areas. The boxes show the 25- and 75-quartile, median values and maximum and minimum values.

4.2.4 Temporal isotopic evolution of snowpack

The open plot isotopic profiles displayed notable variability and changes, predominantly within the middle layer of the snowpack, while the upper layers and the base of the snowpack remained stable. Snowpack loss was the most notable in the middle layer, which demonstrated settling and melt as well as subsequent outflow of meltwater. Furthermore, the disappearance of some upper layers was observed, seemingly without impact on layers below, indicating the formation of preferential path flows paths.

The snow profile conducted on 22 January, demonstrated stratigraphy formed by an isotopically heavier layer on the base of the snowpack, marked F in (Fig.15a), This layer is likely formed by an early snowfall recorded at the beginning of snow accumulation. The isotopically heavier base layer may be typical as the early season snow accumulation occurs at higher atmospheric temperatures than the mid-season snowfall, and isotope values correlate with seasonal temperatures (Rozanski et al., 1992;Evans et al., 2016). This isotopically heavier layer is then followed by isotopically lighter layer labeled E, which is likely result of one of the cold accumulation periods, visible in (Fig.8). This layer is followed by another temporally persistent layer D with high $\delta^{18}O$ and high $\delta^{2}H$. Layers located near the surface demonstrated higher variance in isotopic stratigraphy. The thin layer, labelled C characterized by low $\delta^{18}O$ and $\delta^{2}H$, is located 53cm above the base of the snowpack. This layer is notable for its increased hardness as observed in the physical snow profile (Fig.10). Given that layer C is not observed in other profiles, it may be a result of local snowpack variability. Layer B, found 56cm above the base, is enriched in heavier isotopes compared to layer C as well as to layer A, which forms a surface layer of the 22 January snowpack.

From the second profile conducted on 1 February, loss of the layer A and C is evident while layer E appears to have migrated upwards. Notable is intact isotopic composition of layers B and D exhibiting only minor changes to their $\delta^{18}O$ and $\delta^{2}H$ in response to the melting of the layer A above. The elevated position of layer E higher from the base (now located at 22cm) may be attributed to local topography, where a local depression may have accumulated more snow during the formation of layer F. Similarly, this effect could have been caused by an upward advection induced by snow surface sublimation, which has been suggested to shift the isotopic composition of the snowpack upward (Evans et al., 2016; Gustafson et al., 2010). The occurrence of sublimation may had been possible, given approximately five days of below-zero temperatures with increased net global radiation (Fig.15c) indicating suitable conditions for sublimation (Beria et al., 2018; Earman et al., 2006) . Additionally, the intact layer B indicates that the water produced by the melting of layer A bypassed the underlying layers B and D, potentially refreezing approximately 44 cm above the base and enriching layer D with lighter isotopes. This may be possible due to the below-zero temperatures (0.1 ºC) observed at this snow depth, which is bordered by melt-freeze layers (Fig.15a). The highest recorded $\delta^{18}O$ value was -11.32‰ and the $\delta^{2}H$ value was -80.91‰ in layer D, which bordered by a melt-freeze layer from below, possibly representing a melt front percolating through the adjacent isothermal snowpack.

The upper melt-freeze layer is then observed to disappear on 16 February, which is likely due to the progressive warming of the snowpack, allowing melt front to progress to the second 'lower' melt-freeze layer. Additionally, the disappearance of layer E is evident. This may be result of two potential mechanisms: preferential flow tubes or refreezing, which would result in isotopic the visible isotopic enrichment.

Of note are again the intact layers B, D, and F, despite the loss of snow cover and the ROS events that occurred roughly on 7 and 8 February. The loss of snow cover is more evident in layer D than in the surface layers. The snow cover became increasingly homogeneous between 16 February and 1 March, with isotopic values demonstrating rapid increase. This correlates with the wet snow metamorphism observed in the physical profiles (Fig.11d). The last snow pit revealed an unexpected new, isotopically light, layer at the base of the snowpack, which had not been observed in the previous snow profiles (marked as G in Fig.15a). This layer was probably formed at an earlier point in the season, given that it is found at the very base of the 1 March snowpack. The layer was not observed in other profiles, indicating significant local variability in the open plot snowpack. Moreover, the isotopically lighter layer suggests that the melting of the upper layers did not affect some of the layers below as matrix percolation and refreezing would result in isotopic enrichment of this layer. Comparison with lysimeter data could then provide further insight into the isotopic composition of water leaving the snowpack.

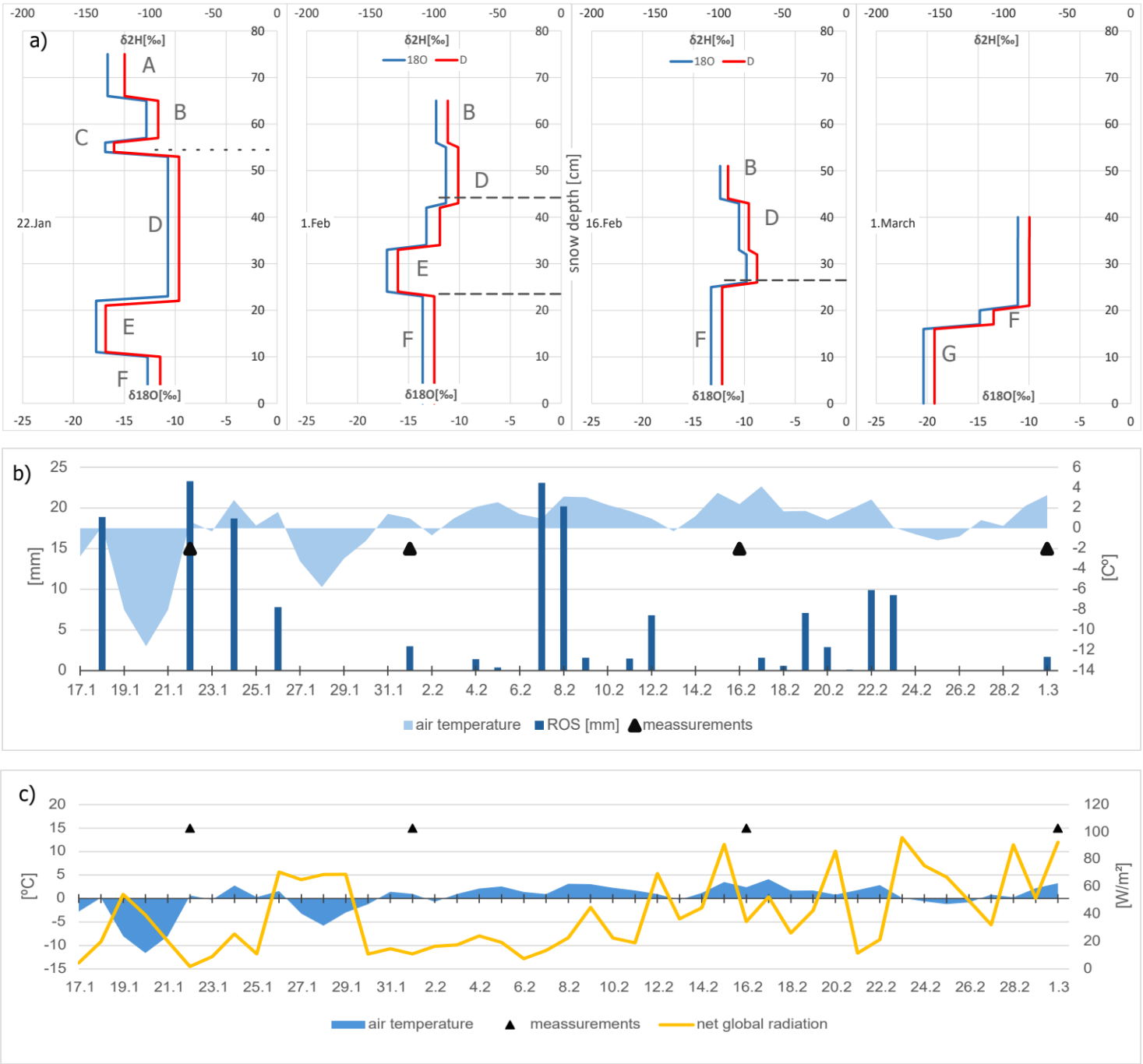

Figure 15: a) The development of isotope ratios 2H/1H and 18O/16O in the snow cover during the winter season of 2024. The height of individual profiles in the graphs corresponds proportionally to the height from the base of the snowpack. The Dotet line indicates a major change in snow hardness, and dashed lines show melt-freeze layers b) Development of temperatures and ROS events during the spam of the measurements. c) Net global radiation with temperatures (data KFGG).

The forest snowpack showed reduced isotopic variance with an enrichment in heavier isotopes in comparison to the snow profiles of the open plots, as ilustrated in (Figure 15). Furthermore, a more linear increase in isotope values was also observed in the forest snowpack. The forest snowpack showed a stable base layer at the bottom of the snowpack, similar to layer F observed in the open plot snowpack. This layer remained relatively intact until 1 February. This isotopically stable layer is consistent with the base layer observed in the physical snow profile, which also exhibited a minimal metamorphic process in comparison to the adjacent upper layers.

The lowest recorded values of δ18O=14.67‰ δ2H=-110.86‰ (Figure 16) were observed in the second snow pit on 1 February. This may indicate the refreezing of surface meltwater, which is enriched in lighter isotopes, in the lower layer or simply by spatial variability. In contrast to the open plot isotopic profiles, the forest snowpack composition appears to be influenced by liquid precipitation or the melting of the surface layers. This indicates more uniform percolation of water through the snowpack. These fractionation processes then resulted in a continuous homogenization and enrichment in heavier isotopes, with the highest values recorded in the last snow cover on 1 March of $\delta^{18}O$= -9.24 $\delta^{2}H$= -65.33. Such isotopic evolution is known as the melt-out effect (Beria et al., 2018).

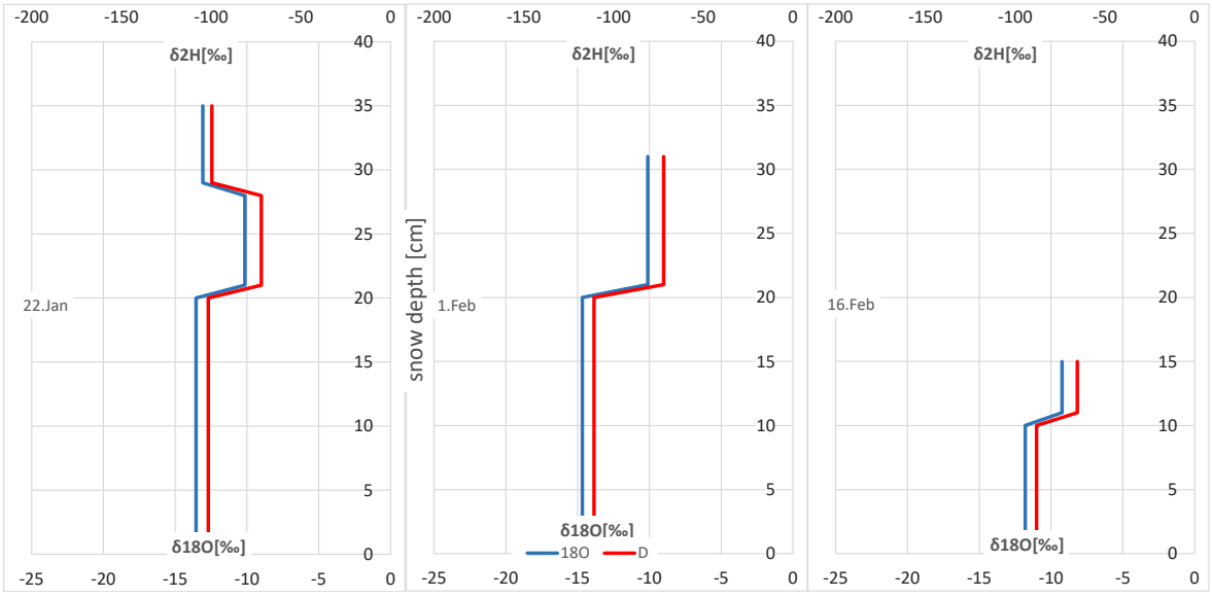

Figure 16: Temporal changes in stable water isotopes $\delta^{18}O$ and $\delta^{2}H$ in the forest snowpack during season 2024.

5 Discussion

5.1 Measurement errors and uncertainties

The findings of this study are potentially subject to uncertainties originating from several sources. General uncertainties could stem from measurement device accuracy and error, or human factors and observer bias. The selected methods for field measurements and data analysis may also introduce a certain degree of uncertainty. Further, the experience and expertise of the researcher are crucial, especially given the subjective nature of certain measures, such as grain type identification, which may be prone to error

Although snow profiles were conducted on the same plot, the specific local topography was not taken into account during the selection of the snow pit. That could have caused different stratigraphy or anomalies in different snow pits. Further, forest edges around the open site may have had a strong influence on snow depths and SWE distribution, as every snow pit on the open plot was at a different distance from the surrounding forest edges. Thus, it could be assumed that surrounding vegetation held a factor in represented data. A comparison with the SPA Snowpack Analyzer station revealed that some physical measurements yielded different snow depths and SWE results than data acquired from the mentioned station, despite their location in the same forest opening. The snow isotopes were sampled from each identified layer of the snowpack, which may have enhanced the correlation between physical and isotopic data. To ensure the independence between the physical and isotopic data, samples could be taken in short regular intervals along the snow profile as done in Evans et al. (2016).

The field measurements are time-consuming and labor-intensive, which makes it challenging to conduct more frequent measurements, which could give more of an inside to the physical and isotopic evolution of the snowpack. The continuity and interpretation of the results are therefore affected by the time interval between the field measurements where different atmospheric conditions could have influenced the snowpack in distinct ways and with different degrees of relevance for the snowpack.

Furthermore, the precipitation data used in this study originates from a nearby meteorological station situated in Modrava, located 5km from the research plot found at an elevation of 1000m above sea level (about 100m meters below the study site). Despite the short distance between the Modrava and our study site, the meteorological conditions may differ at the study site due to different elevations and topography features. Thus, the depicted ROS events and amounts of precipitation may not be in equilibrium at the study site. To address this issue, other measures and variables, such as research site atmospheric temperatures were used to mitigate the impact of these differences in the data. This procedure should ensure no snow precipitation was recorded as a ROS event or vice versa.

5.2 The spatial and temporal variability in snow depth and SWE

The snow physical properties such as snow depth, SWE, grain types, and temperature, were recorded in snow pits located in the open site and the forested site. The forest and open plot snow pits demonstrated a significant difference in almost all mentioned measures. The open site snow pits were reaching snow depths on average 54% higher than the forest sites. Similar results are commonly observed in other studies where sites in a forest opening often accumulate up to 40% more snow than the forested site (Pomeroy et al., 1998; Winkler & Moore, 2006; Jost et al., 2007;). Connaughton (1933b) further reported that the snow depth difference between forest and open sites was amplified in a precipitation low year, where during a light snowfall year forest site accumulated 27,5% less snow than open areas, compared to 4,5% in an average year. This may indicate that snow interception by the canopy played a major role in snow accumulation in the 2024 season. Similar results were obtained for SWE, where open site SWE were on average 36% higher than SWE observed in the forest site. Nearly the same difference in the same area in the Šumava mountains was described by Jenicek, Pevna, et al. (2018) where the SWE in forest sites was on average 40% lower than in the open areas.

Forest plot further showed a linear decline from the first recorded SWE to the complete melt. While on the open plot, both SPA and physically measured data showed more of a fluctuating development, with obvious peaks and consistent minimal values, which did not drop below the initial value (150 mm) until after 16 February. The explanation is likely a snowpack's ability to temporarily store high amounts of water (up to 70%) (Juras et al., 2017). Further Juras et al. (2017) found that a ripe snowpack can withhold substantially more rainwater than a non-ripe snowpack but with higher subsequent meltwater release. Similar water storage patterns were observed by Würzer et al. (2016). The observed SWE fluctuations should therefore be the result of temporary rainwater residence in the snowpack, followed by another ROS event, increasing the snowpack SWE again until the tipping point on the 10th of February, when a continuous decrease of SWE started.

Kattelmann, (1987) then observed that forest snowpacks generated smaller or even no outflow in reaction to ROS events. This could be a result of forest shading of turbulent heat exchanges (Reba et al., 2009; Hotovy & Jenicek, 2020) as well as canopy interception, which generally referred to be up to 50% of the precipitation (Carlyle-Moses & Gash, 2011).

5.3 Physical snow profiles

During the monitored period, a variety of snow profiles with comparable structures were observed beneath the forest canopy and in the open area. The shallower snowpack in the forest plot displayed a smaller amount of physical stratigraphic layers and comparatively weaker vertical temperature gradient. Not a lot of studies have focused on the variability of physical stratigraphic layers between the forest and the open site. Study conducted by Bouchard et al. (2022) showed contrasting results to our findings. The authors of this study observed higher temperature gradients and greater stratigraphic variability under the forest canopy, than in small forest openings in eastern Canada. A similar conclusion was reached in Teich et al. (2019), who reported an increased heterogeneity in stratigraphy on the forest plots affected by MTB outbreak.

Low variability of distinct layers under the forest canopy could be a consequence of a low snowfall winter, resulting in less snowfall intercepted by the forest canopy as snow unloading from the branches has been observed as one of the crucial factors increasing forest snow heterogeneity (Teich et al., 2019). During rain-on-snow events, melt-freeze layers were observed in the open plot snowpack. A similar observation was made in eastern Canada by Bouchard et al. (2022). These melt-freeze layers, then probably altered the rain and meltwater percolation in the open snowpacks as seen in isotope profiles (Fig.15a).

5.4 Snow stable water isotopes

Snow stable water isotope samples from the open plot showed higher variability than samples taken from the plot under the forest canopy. Samples from the open plot varied between $\delta^{18}O$ =-20,37‰; $\delta^{2}H$=154,28‰ and $\delta^{18}O$=-9,79‰; $\delta^{2}H$=-70,09‰. In the forest the values varied between $\delta^{18}O$= -14,67‰; $\delta^{2}H$= -110,86‰ and $\delta^{18}O$=-9,24‰; $\delta^{2}H$=-65,33‰. These values are within the range of $\delta^{18}O$ and $\delta^{2}H$ measured by Holko et al. (2013) in northern Slovakia.

Forest snowpack samples were on average -6,3‰ higher in $\delta^{18}O$ than open plot samples and -46,84‰ higher in $\delta^{2}H$ than on open plot samples. Observations of forest snowpack being more enriched in heavier isotopes were also made by Koeniger et al. (2008), von Freyberg et al. (2020), and Claassen & Downey. (1995). Koeniger et al. (2008) explained the isotopically heavier snow by interception by the forest canopy and subsequent sublimation associated with isotopic enrichment of the remaining snow. An alternative explanation could be isotopic enrichment of canopy intercepted rain entering the snowpack (Beria et al., 2018; Murakami, 2006). Although our results are in general agreement with Koeniger et al. (2008) and von Freyberg et al. (2020), our study found an isotopic difference between the snowpack on open site and the forest site significantly higher than that of von Freyberg et al. (2020) (e.g. 2.3 ‰ in $\delta^{18}O$ and 13.4 ‰ in $\delta^{2}H$), possibly due to generally higher temperatures in the Šumava mountain range during our sampling period. In contrast a study done by Pershin et al. (2023) in

west Siberia found no significant enrichment in heavier isotopes in forest snowpack, due to unsuitable sublimation conditions. This underlines the spatial and temporal variability of the drivers controlling the isotopic fractionation. Study by von Freyberg et al. (2020) hypothesized that, as the results of different studies results seem to show a similar trend, with more experimental data, it might be possible to generalize the isotopic enrichment across catchments with similar vegetation and atmospheric conditions might be possible.

5.5 Snow isotopes profiles evolution

The isotopic profiles demonstrated a different developmental on the open plot compared to the forest. The forest snowpack exhibited a more linear process homogenization and isotopic enrichment during the melting season. This is likely due to the absence of melt-freeze layers, which alter the meltwater percolation (Bouchard et al., 2022), as well as the more stable climate provided by the forest canopy (Hotovy & Jenicek, 2020). In the open plot, the snow profiles showed high $\delta^{18}O$ and $\delta^{2}H$ concentration at the base followed by the isotopically lighter layer and then a layering of relatively enriched snow. Similar observations were also made by Evans et al. (2016) and Zhou et al. (2008). This structure may be a common phenomenon, as precipitation isotopic values correlate with temperatures (Beria et al., 2018). With the progression of the season, samples demonstrated lower variation and an increase in isotopic values (if the last base layer, found on 1 March, is excluded due to its local character). The Process of decreasing heterogeneity and increasing enrichment in heavier isotopes was also observed in Koeniger et al. (2008) or Zhou et al. (2008).

At the open study site, the isotopic stratigraphy demonstrated a notable degree of stability, even after occurrence of ROS events, fluctuations of SWE, and relatively high temperatures during the observed ablation periods. Some layers remained intact, while adjacent layers above melted. This implies the formation of preferential pathways in the upper snowpack, while in the deeper snowpack melt-freeze, layers may border the melt front, preventing the additional melt or rainwater from interfering with layers below (Fig. 15a). These observations are similar to those reported by Evans et al. (2016), in which authors further propose that initial snowpack runoff isotopes, recorded earlier in the season, often represent the upper layers of the snowpack. This results in the snowpack runoff having inverse values of the snowpack's original stratigraphy. Further, Eiriksson et al. (2013) explained the phenomenon of rainwater leaving the snowpack without altering the isotopic composition by lateral flow mechanism. Lateral flow typically occurs in hillslope snowpacks. Given the relatively flat topography of Ptačí brook study site, the observed flow paths can be attributed to lateral lensing, a form of preferential flow (Evans et al., 2016). Furthermore, the occurrence of the isotopically lightest recorded layer on 1 March at the base of the snowpack supports this hypothesis. The usage of lysimeter data could provide more insight into the isotopic composition of snowpack runoff.

6 Conclusion

The thesis provided a comprehensive review of the current scientific literature and research on the physical snow properties related to snowmelt and runoff as well as research methods including the use of stable water isotopes. Additionally, the impacts of climate change and vegetation change on ROS events were examined. Based on the field measurements, we observed the evolution of physical and isotopic stratigraphic layers of snowpack found in the open and forest study plots. Our analysis led us to the following conclusions:

- The first initial hypothesis was confirmed, namely that the SWE is higher on the open plot as well as that the forest plot snowpack has on average higher isotopic values of δ18 O and δ2H. The forest snowpack showed more of a linear homogenization of isotopic composition.

- The SWE on the open plot was, on average, 36 % higher than that observed in the forest plot, with a similarly lower snow depth (54% higher at the open plot). Furthermore, the open area snowpack showed higher stratigraphical heterogeneity.

- The snow stable water isotopes $\delta^{18}O$ and $\delta^{2}H$. showed greater variability at the open site than at the forest site. At the open site, the isotopic values varied between $\delta^{18}O$ =-20,37‰; $\delta^{2}H$=154,28‰ and $\delta^{18}O$=-9,79‰; $\delta^{2}H$=-70,09‰ while at the forest site they isotopic values varied between $\delta^{18}O$= -14,67‰; $\delta^{2}H$= -110,86‰ and $\delta^{18}O$=-9,24‰; $\delta^{2}H$=-65,33‰

- In the open site snowpack, the presence of isotopically persistent layers was observed even after the occurrence of rain events and the melting of approximately half of the initial snowpack. This indicates the occurrence of preferential flow paths in the snowpack, such as lateral lensing.

7 References

Ala-aho, P., Tetzlaff, D., McNamara, J. P., Laudon, H., Kormos, P., & Soulsby, C. (2017). Modeling the isotopic evolution of snowpack and snowmelt: Testing a spatially distributed parsimonious approach. *Water Resources Research*, *53*(7), 5813–5830. https://doi.org/10.1002/2017WR020650

Allard, W. (1957). Snow Hydrology: Summary Report of the Snow Investigations. Published by the North Pacific Division, Corps of Engineers, U.S. Army, Portland, Oregon, 1956. 437 pages, 70 pages of plates, maps and figs., 27 cm. * . *Journal of Glaciology*, *3*(22), 148-148. https://doi.org/10.3189/s0022143000024503

Andreadis, K. M., Storck, P., & Lettenmaier, D. P. (2009). Modeling snow accumulation and ablation processes in forested environments. *Water Resources Research*, *45*(5). https://doi.org/10.1029/2008WR007042

Avanzi, F., Yamaguchi, S., Hirashima, H., & De Michele, C. (2015). Bulk volumetric liquid water content in a seasonal snowpack: Modeling its dynamics in different climatic conditions. *Advances in Water Resources*, *86, 1-13*. https://doi.org/10.1016/j.advwatres.2015.09.021

Baggi, S., & Schweizer, J. (2009). Characteristics of wet-snow avalanche activity: 20 years of observations from a high alpine valley (Dischma, Switzerland). *Natural Hazards*, *50*(1), 97-108. https://doi.org/10.1007/s11069-008-9322-7

Barnett, T. P., Adam, J. C., & Lettenmaier, D. P. (2005). Potential impacts of a warming climate on water availability in snow-dominated regions. In *Nature* 438(7066), 303-309. https://doi.org/10.1038/nature04141

Bartík, M., Holko, L., Jančo, M., Škvarenina, J., Danko, M., & Kostka, Z. (2019). Influence of mountain spruce forest dieback on snow accumulation and melt. *Journal of Hydrology and Hydromechanics*, *67*(1), 59-69. https://doi.org/10.2478/johh-2018-0022

Beniston, M., Farinotti, D., Stoffel, M., Andreassen, L. M., Coppola, E., Eckert, N., Fantini, A., Giacona, F., Hauck, C., Huss, M., Huwald, H., Lehning, M., López-Moreno, J. I., Magnusson, J., Marty, C., Morán-Tejéda, E., Morin, S., Naaim, M., Provenzale, A., … Vincent, C. (2018). The European mountain cryosphere: A review of its current state, trends, and future challenges. In *Cryosphere* 12(2), 759-794. https://doi.org/10.5194/tc-12-759-2018

Beria, H., Larsen, J. R., Ceperley, N. C., Michelon, A., Vennemann, T., & Schaefli, B. (2018). Understanding snow hydrological processes through the lens of stable

water isotopes. *Wiley Interdisciplinary Reviews: Water*, *5*(6),e1311. https://doi.org/10.1002/wat2.1311

Biederman, J. A., Harpold, A. A., Gochis, D. J., Ewers, B. E., Reed, D. E., Papuga, S. A., & Brooks, P. D. (2014). Increased evaporation following widespread tree mortality limits streamflow response. Water Resources Research, 50(7), 5395-5409. http://doi.org/10.1002/2013WR014994

Blöschl, G., Bierkens, M. F. P., Chambel, A., Cudennec, C., Destouni, G., Fiori, A., Kirchner, J. W., McDonnell, J. J., Savenije, H. H. G., Sivapalan, M., Stumpp, C., Toth, E., Volpi, E., Carr, G., Lupton, C., Salinas, J., Széles, B., Viglione, A., Aksoy, H., … Zhang, Y. (2019). Twenty-three unsolved problems in hydrology (UPH)–a community perspective. Hydrological Sciences Journal, 64(10), 1141-1158. http://doi.org/10.1080/02626667.2019.1620507

Bouchard, B., Nadeau, D. F., & Domine, F. (2022). Comparison of snowpack structure in gaps and under the canopy in a humid boreal forest. Hydrological Processes, 36(9), e14681. http://doi.org/10.1002/hyp.14681

Bouvet, L., Calonne, N., Flin, F., & Geindreau, C. (2022). Snow Equi-Temperature Metamorphism Described by a Phase-Field Model Applicable on Micro-Tomographic Images: Prediction of Microstructural and Transport Properties. Journal of Advances in Modeling Earth Systems, 14(9), e2022MS002998. http://doi.org/10.1029/2022ms002998

Brandt, W. T., Haleakala, K., Hatchett, B. J., & Pan, M. (2022). A Review of the Hydrologic Response Mechanisms During Mountain Rain-on-Snow. Frontiers in Earth Science, 10, 791760. http://doi.org/10.3389/feart.2022.791760

Cane, G., & Clark, I. D. (1999). Tracing ground water recharge in an agricultural watershed with isotopes. Ground Water, 37(1), 133-139. http://doi.org/10.1111/j.1745-6584.1999.tb00966.x

Carlyle-Moses, D. E., & Gash, J. H. C. (2011). Rainfall Interception Loss by Forest Canopies. In D. F. Levia, D. E. Carlyle-Moses, & T. Tanaka (Eds.), Forest Hydrology and Biogeochemistry: Synthesis of Past Research and Future Directions (pp. 407-432). Springer. http://doi.org/10.1007/978-94-007-1363-5_20

Carroll, R. W. H., Deems, J., Maxwell, R., Sprenger, M., Brown, W., Newman, A., Beutler, C., Bill, M., Hubbard, S. S., & Williams, K. H. (2022). Variability in observed stable water isotopes in snowpack across a mountainous watershed in Colorado. Hydrological Processes, 36(8), e14653. http://doi.org/10.1002/hyp.14653

Cherkauer, K. A., Bowling, L. C., & Lettenmaier, D. P. (2003). Variable infiltration capacity cold land process model updates. Global and Planetary Change, 38(1–2), 151-159. http://doi.org/10.1016/S0921-8181(03)00025-0

Claassen, H. C., & Downey, J. S. (1995). A Model for Deuterium and Oxygen 18 Isotope Changes During Evergreen Interception of Snowfall. Water Resources Research, 31(3), 601-618. http://doi.org/10.1029/94WR01995

Clark, M. J., & Seppala, M. (1988). Slushflows in a subarctic environment, Kilpisjarvi, Finnish Lapland. Arctic & Alpine Research, 20(1), 97-105. https://doi.org/10.1080/00040851.1988.12002655

DeWalle, D. R., & Rango, A. (2008). Principles of snow hydrology. In Principles of Snow Hydrology (Vol. 9780521823623). http://doi.org/10.1017/CBO9780511535673

Dietz, A. J., Kuenzer, C., Gessner, U., & Dech, S. (2012). Remote sensing of snow - a review of available methods. International Journal of Remote Sensing, 33(13), 4094-4134. http://doi.org/10.1080/01431161.2011.640964

Earman, S., Campbell, A. R., Phillips, F. M., & Newman, B. D. (2006). Isotopic exchange between snow and atmospheric water vapor: Estimation of the snowmelt component of groundwater recharge in the southwestern United States. Journal of Geophysical Research Atmospheres, 111(D9). http://doi.org/10.1029/2005JD006470

Eiriksson, D., Whitson, M., Luce, C. H., Marshall, H. P., Bradford, J., Benner, S. G., Black, T., Hetrick, H., & McNamara, J. P. (2013). An evaluation of the hydrologic relevance of lateral flow in snow at hillslope and catchment scales. Hydrological Processes, 27(5), 640-654. http://doi.org/10.1002/hyp.9666

Essery, R., Pomeroy, J., Parviainen, J., & Storck, P. (2003). Sublimation of snow from coniferous forests in a climate model. Journal of Climate, 16(11), 1855-1864. http://doi.org/10.1175/1520-0442(2003)016<1855>2.0.CO;2

Evans, S. L., Flores, A. N., Heilig, A., Kohn, M. J., Marshall, H. P., & McNamara, J. P. (2016). Isotopic evidence for lateral flow and diffusive transport, but not sublimation, in a sloped seasonal snowpack, Idaho, USA. Geophysical Research Letters, 43(7), 3298-3306. http://doi.org/10.1002/2015GL067605

Fierz, C., Armstrong, R. L., Durand, Y., Etchevers, P., Greene, E., McClung, D. M., Nishimura, K., Satyawali, P. K., & Sokratov, S. A. (2009). The international classification for seasonal snow on the ground. In UNESCO, IHP–VII, Technical Documents in Hydrology, No 83; IACS contribution No 1.

Garvelmann, J., Pohl, S., & Weiler, M. (2014). Variability of observed energy fluxes during rain-on-snow and clear sky snowmelt in a midlatitude mountain environment. *Journal of Hydrometeorology*, *15*(3) ,1220-1237. https://doi.org/10.1175/JHM-D-13-0187.1

Gelfan, A. N., Pomeroy, J. W., & Kuchment, L. S. (2004). Modeling forest cover influences on snow accumulation, sublimation, and melt. *Journal of*

Hydrometeorology, *5*(5), 785-803. https://doi.org/10.1175/1525-7541(2004)005<0785:MFCIOS>2.0.CO;2

Gouttevin, I., Lehning, M., Jonas, T., Gustafsson, D., & Mölder, M. (2015). A two-layer canopy model with thermal inertia for an improved snowpack energy balance below needleleaf forest (model SNOWPACK, version 3.2.1, revision 741). *Geoscientific Model Development*, *8*(8), 2379-2398. https://doi.org/10.5194/gmd-8-2379-2015

Gustafson, J. R., Brooks, P. D., Molotch, N. P., & Veatch, W. C. (2010). Estimating snow sublimation using natural chemical and isotopic tracers across a gradient of solar radiation. *Water Resources Research*, *46*(12). https://doi.org/10.1029/2009WR009060

Hannah, D. M., Brown, L. E. E. E., & Milner, A. M. (2007). CASE STUDIES AND REVIEWS Integrating climate – hydrology – ecology for alpine river systems. *Aquatic Conservation: Marine and Freshwater Ecosystems*, *656*(October 2006). https://doi.org/10.1002/aqc

Hirashima, H., Yamaguchi, S., Sato, A., & Lehning, M. (2010). Numerical modeling of liquid water movement through layered snow based on new measurements of the water retention curve. *Cold Regions Science and Technology*, *64*(2), 94-103. https://doi.org/10.1016/j.coldregions.2010.09.003

Hock, R. (1999). A distributed temperature-index ice- and snowmelt model including potential direct solar radiation. *Journal of Glaciology*, *45*(149), 101-111. https://doi.org/10.1017/S0022143000003087

Hock, R. (2003). Temperature index melt modelling in mountain areas. *Journal of Hydrology*, *282*(1–4), 104-115. https://doi.org/10.1016/S0022-1694(03)00257-9

Holko, L., Danko, M., Dóša, M., Kostka, Z., Šanda, M., Pfister, L., & Iffly, J. F. (2013). Spatial and temporal variability of stable water isotopes in snow related hydrological processes. *Bodenkultur*, *64*(3–4), 39-45.

Hotovy, O., & Jenicek, M. (2020). The impact of changing subcanopy radiation on snowmelt in a disturbed coniferous forest. *Hydrological Processes*, *34*(26), 5298-5314. https://doi.org/10.1002/hyp.13936

Ishida, K., Ohara, N., Ercan, A., Jang, S., Trinh, T., Kavvas, M. L., Carr, K., & Anderson, M. L. (2019). Impacts of climate change on snow accumulation and melting processes over mountainous regions in Northern California during the 21st century. *Science of the Total Environment*, *685, 104-115*. https://doi.org/10.1016/j.scitotenv.2019.05.255

Ismail, M. F., Bogacki, W., Disse, M., Schäfer, M., & Kirschbauer, L. (2023). Estimating degree-day factors of snow based on energy flux components. *Cryosphere*, *17*(1), 211-231. https://doi.org/10.5194/tc-17-211-2023

Jamieson, B. (2006). Formation of refrozen snowpack layers and their role in slab avalanche release. *Reviews of Geophysics*, *44*(2). https://doi.org/10.1029/2005RG000176

Jenicek, M., Hnilica, J., Nedelcev, O., & Sipek, V. (2021). Future changes in snowpack will impact seasonal runoff and low flows in Czechia. *Journal of Hydrology: Regional Studies*, *37, 100899*. https://doi.org/10.1016/j.ejrh.2021.100899

Jeníček, M., Hotový, O., & Matějka, O. (2017). Snow accumulation and ablation in different canopy structures at a plot scale: Using degree-day approach and measured shortwave radiation. *Acta Universitatis Carolinae, Geographica*, *52*(1), 61-72. https://doi.org/10.14712/23361980.2017.5

Jenicek, M., Pevna, H., & Matejka, O. (2018). Canopy structure and topography effects on snow distribution at a catchment scale: Application of multivariate approaches. *Journal of Hydrology and Hydromechanics*, *66*(1), 43-54. https://doi.org/10.1515/johh-2017-0027

Jenicek, M., Seibert, J., & Staudinger, M. (2018). Modeling of Future Changes in Seasonal Snowpack and Impacts on Summer Low Flows in Alpine Catchments. *Water Resources Research*, *54*(1), 538-556. https://doi.org/10.1002/2017WR021648

Jennings, K. S., Kittel, T. G. F., & Molotch, N. P. (2018). Observations and simulations of the seasonal evolution of snowpack cold content and its relation to snowmelt and the snowpack energy budget. *Cryosphere*, *12*(5), 1595-1614. https://doi.org/10.5194/tc-12-1595-2018

Jennings, K. S., & Molotch, N. P. (2020). Snowfall Fraction, Cold Content, and Energy Balance Changes Drive Differential Response to Simulated Warming in an Alpine and Subalpine Snowpack. *Frontiers in Earth Science*, *8,* 186*.* https://doi.org/10.3389/feart.2020.00186

Jost, G., Weiler, M., Gluns, D. R., & Alila, Y. (2007). The influence of forest and topography on snow accumulation and melt at the watershed-scale. *Journal of Hydrology*, *347*(1–2), 101-115. https://doi.org/10.1016/j.jhydrol.2007.09.006

Juras, R., Blöcher, J. R., Jenicek, M., Hotovy, O., & Markonis, Y. (2021). What affects the hydrological response of rain-on-snow events in low-altitude mountain ranges in Central Europe? *Journal of Hydrology*, *603, 127002*. https://doi.org/10.1016/j.jhydrol.2021.127002

Juras, R., Pavlásek, J., Vitvar, T., Šanda, M., Holub, J., Jankovec, J., & Linda, M. (2016). Isotopic tracing of the outflow during artificial rain-on-snow event. *Journal of Hydrology*, *541, 1145-1154*. https://doi.org/10.1016/j.jhydrol.2016.08.018

Juras, R., Würzer, S., Pavlásek, J., Vitvar, T., & Jonas, T. (2017). Rainwater propagation through snowpack during rain-on-snow sprinkling experiments under

different snow conditions. *Hydrology and Earth System Sciences*, *21*(9), 4973-4987. https://doi.org/10.5194/hess-21-4973-2017

Kattelmann, R. (1987). Water release from a forested snowpack during rainfall. *Forest Hydrology and Watershed Management - IAHS Publication*, *167*.

Klaus, J., & McDonnell, J. J. (2013). Hydrograph separation using stable isotopes: Review and evaluation. In *Journal of Hydrology* 505, 47-64. https://doi.org/10.1016/j.jhydrol.2013.09.006

Koeniger, P., Hubbart, J. A., Link, T., & Marshall, J. D. (2008). Isotopic variation of snow cover and streamflow in response to changes in canopy structure in a snow-dominated mountain catchment. *Hydrological Processes*, *22*(4) 557-566. https://doi.org/10.1002/hyp.6967

Lackner, G., Domine, F., Nadeau, D. F., Parent, A. C., Anctil, F., Lafaysse, M., & Dumont, M. (2022). On the energy budget of a low-Arctic snowpack. *Cryosphere*, *16*(1), 127-142. https://doi.org/10.5194/tc-16-127-2022

Langhammer, J., Su, Y., & Bernsteinová, J. (2015). Runoff response to climate warming and forest disturbance in a mid-mountain basin. *Water (Switzerland)*, *7*(7), 3320-3342. https://doi.org/10.3390/w7073320

Li, D., Lettenmaier, D. P., Margulis, S. A., & Andreadis, K. (2019). The Role of Rain-on-Snow in Flooding Over the Conterminous United States. *Water Resources Research*, *55*(11), 8492-8513. https://doi.org/10.1029/2019WR024950

Lu, H. (2012). Changes in seasonal snow liquid water content during the snowmelt period in the Western Tianshan Mountains, China. *The Cryosphere Discussions*, *6*(5) 4137-4169. https://doi.org/10.5194/tcd-6-4137-2012

Lundquist, J. D., Dickerson-Lange, S. E., Lutz, J. A., & Cristea, N. C. (2013). Lower forest density enhances snow retention in regions with warmer winters: A global framework developed from plot-scale observations and modeling. *Water Resources Research*, *49*(10), 6356-6370. https://doi.org/10.1002/wrcr.20504

Marshall, A. M., Link, T. E., Robinson, A. P., & Abatzoglou, J. T. (2020). Higher Snowfall Intensity is Associated with Reduced Impacts of Warming Upon Winter Snow Ablation. *Geophysical Research Letters*, *47*(4), e2019GL086409. https://doi.org/10.1029/2019GL086409

Marty, C., Schlögl, S., Bavay, M., & Lehning, M. (2017). How much can we save? Impact of different emission scenarios on future snow cover in the Alps. *Cryosphere*, *11*(1), 517-529. https://doi.org/10.5194/tc-11-517-2017

McCabe, G. J., Clark, M. P., & Hay, L. E. (2007). Rain-on-snow events in the western United States. *Bulletin of the American Meteorological Society*, *88*(3), 319-328. https://doi.org/10.1175/BAMS-88-3-319

Morán-Tejeda, E., López-Moreno, J. I., & Beniston, M. (2013). The changing roles of temperature and precipitation on snowpack variability in Switzerland as a function of altitude. *Geophysical Research Letters*, *40*(10), 2131-2136. https://doi.org/10.1002/grl.50463

Mosier, T. M., Hill, D. F., & Sharp, K. V. (2016). How much cryosphere model complexity is just right? Exploration using the conceptual cryosphere hydrology framework. *Cryosphere*, *10*(5), 2147-2171. https://doi.org/10.5194/tc-10-2147-2016

Mudryk, L. R., Kushner, P. J., Derksen, C., & Thackeray, C. (2017). Snow cover response to temperature in observational and climate model ensembles. *Geophysical Research Letters*, *44*(2), 919-926. https://doi.org/10.1002/2016GL071789

Murakami, S. (2006). A proposal for a new forest canopy interception mechanism: Splash droplet evaporation. *Journal of Hydrology*, *319*(1–4) 72-82. https://doi.org/10.1016/j.jhydrol.2005.07.002

Musselman, K. N., Clark, M. P., Liu, C., Ikeda, K., & Rasmussen, R. (2017). Slower snowmelt in a warmer world. *Nature Climate Change*, *7*(3), 214-219. https://doi.org/10.1038/nclimate3225

Musselman, K. N., Lehner, F., Ikeda, K., Clark, M. P., Prein, A. F., Liu, C., Barlage, M., & Rasmussen, R. (2018). Projected increases and shifts in rain-on-snow flood risk over western North America. In *Nature Climate Change* 8(9), 808-812. https://doi.org/10.1038/s41558-018-0236-4

Nakaya, U. (1954). Snow Crystals: Natural and Artificial. *Science*, *120*(3123). https://doi.org/10.4159/harvard.9780674182769.c9

Overpeck, J. T., Rind, D., & Goldberg, R. (1990). Climate-induced changes in forest disturbance and vegetation. *Nature*, *343*(6253), 51-53. https://doi.org/10.1038/343051a0

Pellicciotti, F., Brock, B., Strasser, U., Burlando, P., Funk, M., & Corripio, J. (2005). An enhanced temperature-index glacier melt model including the shortwave radiation balance: Development and testing for Haut Glacier d'Arolla, Switzerland. *Journal of Glaciology*, *51*(175), 573-587. https://doi.org/10.3189/172756505781829124

Pershin, D., Malygina, N., Chernykh, D., Biryukov, R., Zolotov, D., & Lubenets, L. (2023). Variability in Snowpack Isotopic Composition between Open and Forested Areas in the West Siberian Forest Steppe. *Forests*, *14*(1), 160. https://doi.org/10.3390/f14010160

Pomeroy, J. W., Parviainen, J., Hedstrom, N., & Gray, D. M. (1998). Coupled modelling of forest snow interception and sublimation. *Hydrological Processes*, *12*(15),

2317-2337. https://doi.org/10.1002/(SICI)1099-1085(199812)12:15<2317::AID-HYP799>3.0.CO;2-X

Pomeroy, J. W., Stewart, R. E., & Whitfield, P. H. (2016). The 2013 flood event in the South Saskatchewan and Elk River basins: Causes, assessment and damages. *Canadian Water Resources Journal*, *41*(1–2), 105-117. https://doi.org/10.1080/07011784.2015.1089190

Rango, A., & Martinec, J. (1995). REVISITING THE DEGREE-DAY METHOD FOR SNOWMELT COMPUTATIONS. *JAWRA Journal of the American Water Resources Association*, *31*(4), 657-669. https://doi.org/10.1111/j.1752-1688.1995.tb03392.x

Rozanski, K., Araguás-Araguás, L., & Gonfiantini, R. (1992). Relation Between Long-Term Trends of Oxygen-18 Isotope Composition of Precipitation and Climate. *Science*, *258*(5084), 981-985. https://doi.org/10.1126/science.258.5084.981

Schürch, M., Kozel, R., Schotterer, U., & Tripet, J. P. (2003). Observation of isotopes in the water cycle - The Swiss National Network (NISOT). In *Environmental Geology* 45(1), 1-11. https://doi.org/10.1007/s00254-003-0843-9

Seibert, J., Jenicek, M., Huss, M., & Ewen, T. (2015a). Snow and Ice in the Hydrosphere. In *Snow and Ice-Related Hazards, Risks, and Disasters*. (pp. 93-135). https://doi.org/10.1016/B978-0-12-394849-6.00004-4

Seibert, J., Jenicek, M., Huss, M., & Ewen, T. (2015b). Snow and Ice in the Hydrosphere. In *Snow and Ice-Related Hazards, Risks, and Disasters*. (pp. 93-135). Elsevier. https://doi.org/10.1016/B978-0-12-394849-6.00004-4

Sharp, Z. (2017). Principles of Stable Isotope Geochemistry, 2nd edition. *Principles of Stable Isotope Geochemistry, 2nd Edition*, *136*(1). https://doi.org/10.25844/h9q1-0p82

Stewart, I. T., Cayan, D. R., & Dettinger, M. D. (2004). Changes in snowmelt runoff timing in western North America under a “business as usual” climate change scenario. *Climatic Change*, *62*(1–3), 217-232. https://doi.org/10.1023/B:CLIM.0000013702.22656.e8

Sui, J., Koehler, G., & Krol, F. (2010). Characteristics of rainfall, snowmelt and runoff in the headwater region of the main river watershed in Germany. *Water Resources Management*, *24*(10), 2167-2186. https://doi.org/10.1007/s11269-009-9545-8

Surfleet, C. G., & Tullos, D. (2013). Variability in effect of climate change on rain-on-snow peak flow events in a temperate climate. *Journal of Hydrology*, *479*, 24–34. https://doi.org/10.1016/j.jhydrol.2012.11.021

Svoboda, V., Hanel, M., Máca, P., & Kyselý, J. (2016). Projected changes of rainfall event characteristics for the Czech Republic. *Journal of Hydrology and Hydromechanics*, *64*(4), 415-425. https://doi.org/10.1515/johh-2016-0036

Taylor, S., Feng, X., Kirchner, J. W., Osterhuber, R., Klaue, B., & Renshaw, C. E. (2001). Isotopic evolution of a seasonal snowpack and its melt. *Water Resources Research*, *37*(3) 759-769. https://doi.org/10.1029/2000WR900341

Teich, M., Giunta, A. D., Hagenmuller, P., Bebi, P., Schneebeli, M., & Jenkins, M. J. (2019). Effects of bark beetle attacks on forest snowpack and avalanche formation – Implications for protection forest management. *Forest Ecology and Management*, *438, 186-203*. https://doi.org/10.1016/j.foreco.2019.01.052

Thackeray, C. W., Derksen, C., Fletcher, C. G., & Hall, A. (2019). Snow and Climate: Feedbacks, Drivers, and Indices of Change. In *Current Climate Change Reports* 5(4), 322-333. https://doi.org/10.1007/s40641-019-00143-w

Varhola, A., Coops, N. C., Weiler, M., & Moore, R. D. (2010). Forest canopy effects on snow accumulation and ablation: An integrative review of empirical results. In *Journal of Hydrology* 392(3–4) ,219-233. https://doi.org/10.1016/j.jhydrol.2010.08.009

Veatch, W., Brooks, P. D., Gustafson, J. R., & Molotch, N. P. (2009). “Quantifying the effects of forest canopy cover on net snow accumulation at a continental, mid-latitude site.” *Ecohydrology*, *2*(2), 115-128. https://doi.org/10.1002/eco.45

von Freyberg, J., Bjarnadóttir, T. R., & Allen, S. T. (2020). Influences of forest canopy on snowpack accumulation and isotope ratios. *Hydrological Processes*, *34*(3), 679-690. https://doi.org/10.1002/hyp.13617

Walsh, E. S., Vierling, K. T., Strand, E., Bartowitz, K., & Hudiburg, T. W. (2019). Climate change, woodpeckers, and forests: Current trends and future modeling needs. In *Ecology and Evolution* 9(4), 2305-2319. https://doi.org/10.1002/ece3.4876

Wayand, N. E., Lundquist, J. D., & Clark, M. P. (2015). Modeling the influence of hypsometry, vegetation, and storm energy on snowmelt contributions to basins during rain-on-snow floods. *Water Resources Research*, *51*(10), 8551-8569. https://doi.org/10.1002/2014WR016576

Winkler, R. D., & Moore, R. D. (2006). Variability in snow accumulation patterns within forest stands on the interior plateau of British Columbia, Canada. *Hydrological Processes*, *20*(17), 3683-3695. https://doi.org/10.1002/hyp.6382

Würzer, S., Jonas, T., Wever, N., & Lehning, M. (2016). Influence of initial snowpack properties on runoffformation during rain-on-snow events. *Journal of Hydrometeorology*, *17*(6), 1801-1815. https://doi.org/10.1175/JHM-D-15-0181.1

Zeng, X., Broxton, P., & Dawson, N. (2018). Snowpack Change From 1982 to 2016 Over Conterminous United States. *Geophysical Research Letters*, *45*(23), 12-940. https://doi.org/10.1029/2018GL079621

Zhou, S., Nakawo, M., Hashimoto, S., & Sakai, A. (2008). The effect of refreezing on the isotopic composition of melting snowpack. *Hydrological Processes*, *22*(6), 873-882. https://doi.org/10.1002/hyp.6662

Digital sources:

ČÚZK. (2016). ZABAGED® - Výškopis - DMR 5G. Digitální model reliéfu České republiky 5. generace v S-JTSK, Bpv. Mapový podklad © Český úřad zeměměřický a katastrální. Retrieved July 29, 2024, from https://www.cuzk.cz/

ČÚZK. (2020). Ortofoto České republiky. Retrieved July 25, 2024, from https://www.cuzk.cz/

ČHMÚ. (2023). Český hydrometeorologický ústav. Retrieved July 25, 2024, from https://www.chmi.cz/

Copernicus Land Monitoring Service. (2018). Dominant Leaf Type 2018 (raster 10 m), Europe, 3-yearly. Retrieved July 25, 2024, from http://www.land.copernicus.eu

DIBAVOD. (2022). Digitální báze vodohospodářských dat. VÚV TGM. Retrieved July 25, 2024, from https://www.dibavod.cz/

niViz. (2024). Interactive Visualization of Snow Profiles and Auxiliary Data [software]. Retrieved July 25, 2024, from http://www.niviz.org

8 List of figures

9 List of tables

10 Appendices

Appendix 1: Snow profiles on the open site

Location: Open site 1 February

Date / Time: 2024-02-01 12:00 +02:00

Observer:	Altitude: -- m	Air temp.:
Profilenr:	Exposition: n/a	Cloudiness:
	Coordinates: --	Wind:
Snow height: 65 cm (SWE: 262 kg/m²)	Avg. density: 403 kg/m³	Avg. ram resistance:
Hasty Pit: No		

Remarks:

● RGlr ○ Melf forms (MF) MFpc MFcl

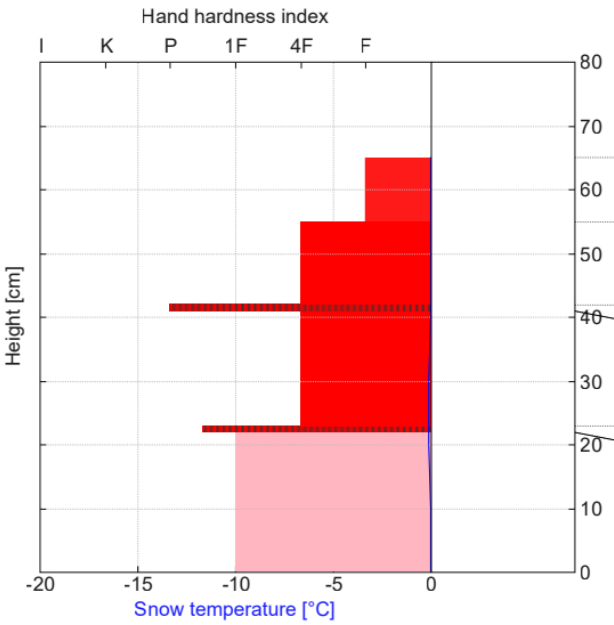

θ	F	E mm	R	ρ kg/m³
	MFpc	3	1	480
	MFpc	1.5 - 2	2	385
	MFcl	0.5	4	505
	MFpc	1.5	2	
	MFcl	0.5	3.5	296
	●	1	3	

Location: Open site 16 February | **Date / Time: 2024-02-16 10:37 +02:00**

Observer: | Altitude: -- m | Air temp.:

Profilenr: | Exposition: n/a | Cloudiness:

Coordinates: -- | Wind:

Snow height: 51 cm (SWE: 202 kg/m²) | Avg. density: 396 kg/m³ | Avg. ram resistance:

Hasty Pit: No

Remarks:

● RGlr ○ Melf forms (MF) MFpc MFcl

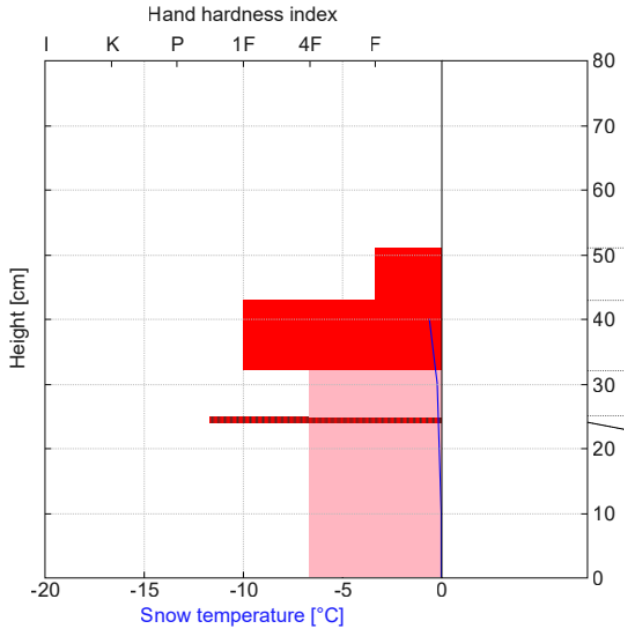

θ	F	E mm	R	ρ kg/m³
	MFpc	3	1	375
	MFpc	1	3	491
	●(MFpc)	1	2	943
	MFcl	0.5	3.5	208
	●(○)	1	2	

Location: Open site 1 March
Observer:
Profilenr:

Altitude: -- m
Exposition: n/a
Coordinates: --

Date / Time: 2024-03-01 13:07 +02:00
Air temp.:
Cloudiness:
Wind:

Snow height: 40 cm (SWE: 159 kg/m²)
Hasty Pit: No

Avg. density: 398 kg/m³
Avg. ram resistance:

Remarks:

● RGlr ♈ MFpc

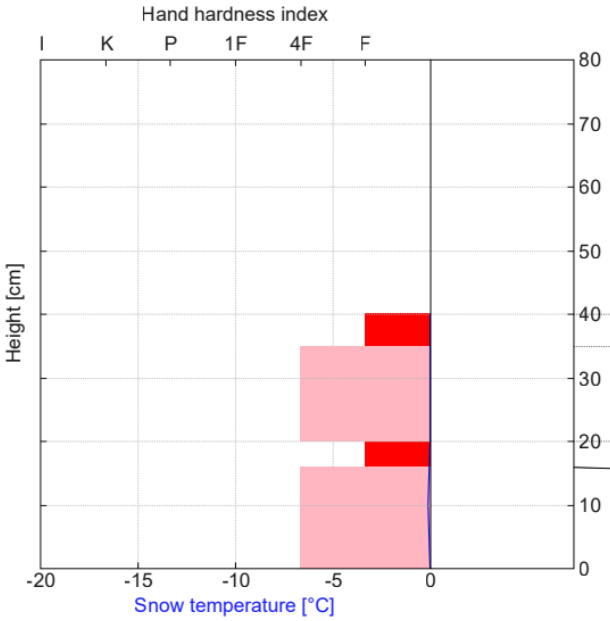

θ	F	E mm	R	ρ kg/m³
	♈		1	520
	●	0.5	2	347
	♈	2	1	475
	●	0.5	2	388

Appendix 2: Forest snow profiles:

7/29/24, 10:16 PM SL_2.caaml

Location: Forest site 22 January **Date / Time: 2024-01-22 12:00 +02:00**

Observer:	Altitude: -- m	Air temp.:
Profilenr:	Exposition: n/a	Cloudiness:
	Coordinates: --	Wind:
Snow height: 38 cm (SWE: 114 kg/m²)	Avg. density: 300 kg/m³	Avg. ram resistance:
Hasty Pit: No		

Remarks:

● Rounded grains (RG) □ Faceted crystals (FC)

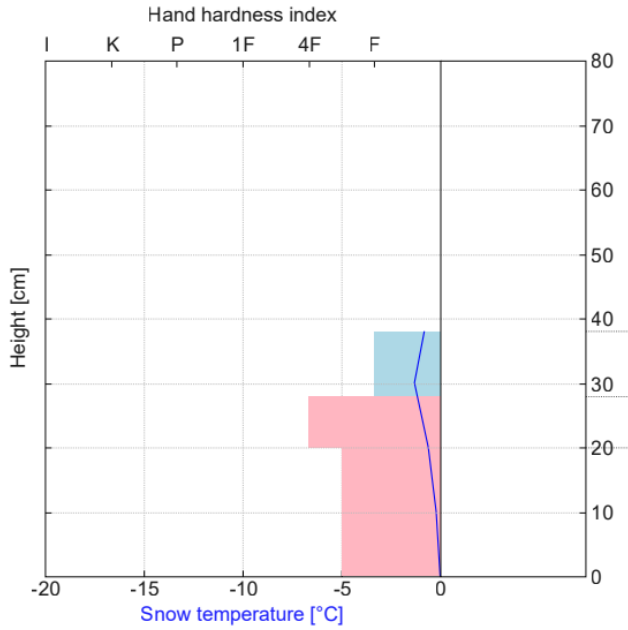

θ	F	E mm	R	ρ kg/m³
	□(●)	1 - 2	1	280
	●	1	2	300
	●	1	1.5	310

Location: Fores site 1 February **Date / Time: 2024-02-01 12:10 +02:00**

Observer:	Altitude: -- m	Air temp.:
	Exposition:	Cloudiness:
	Coordinates: --	Wind:
Snow height: 31 cm (SWE: 90 kg/m²)	Avg. density: 290 kg/m³	Avg. ram resistance:

● Rounded grains (RG) ○ Melf forms (MF)

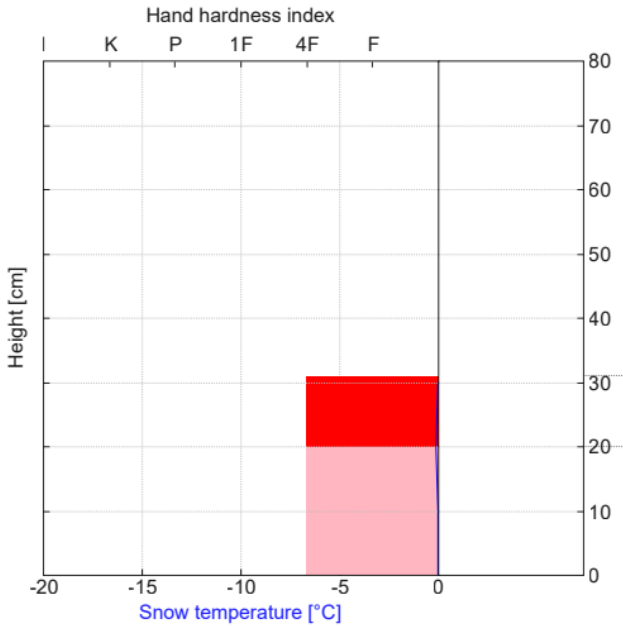

θ	F	E mm	R	ρ kg/m³
	○	2	2	382
	●	1	2	240

Location: Forest site 16 February **Date / Time: 2024-02-16 12:13 +02:00**

Observer:	Altitude: -- m	Air temp.:
	Exposition:	Cloudiness:
	Coordinates: --	Wind:
Snow height: 15 cm	Avg. density: --	Avg. ram resistance:

o Melf forms (MF)

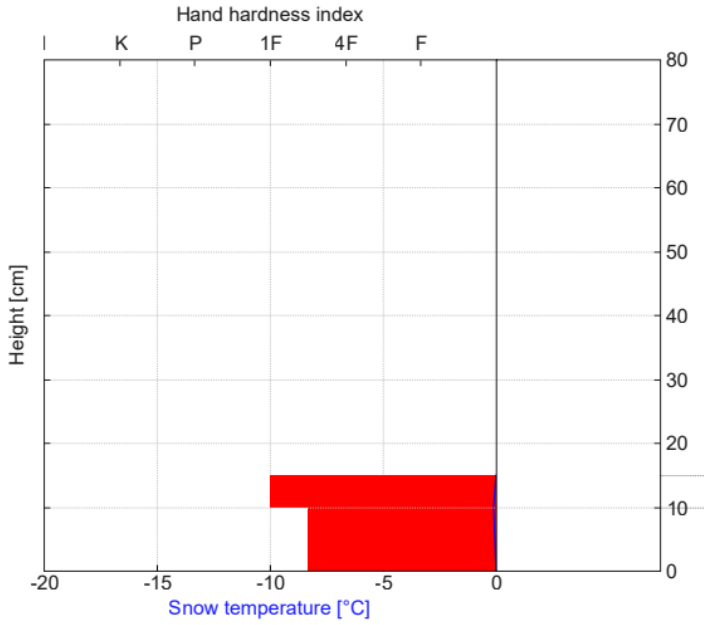

θ	F	E mm	R
	o	2	3
	o	0.5	2.5